



Structure-property relationships of functional materials

Tim Kodalle

Team Lead – Lawrence Berkeley National Laboratory
(Molecular Foundry and Advanced Light Source)

05.09.2025



timkodalle@lbl.gov



Combining characterization and synthesis facilities



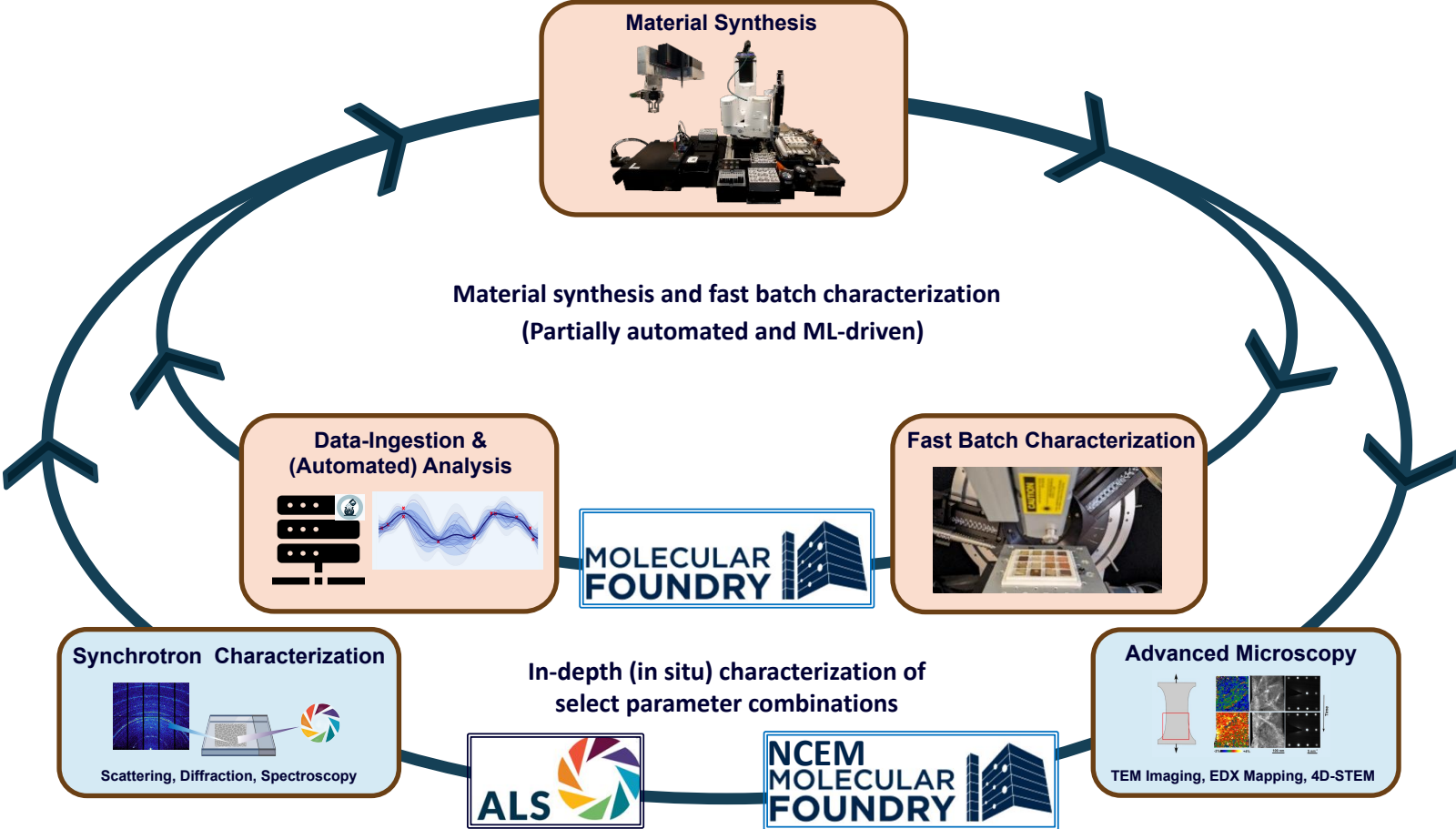
Berkeley Lab's synchrotron light source

- In situ XRD during thin-film synthesis (BL 12.3.2)
- In situ, high-temperature pXRD (BL 12.2.2)

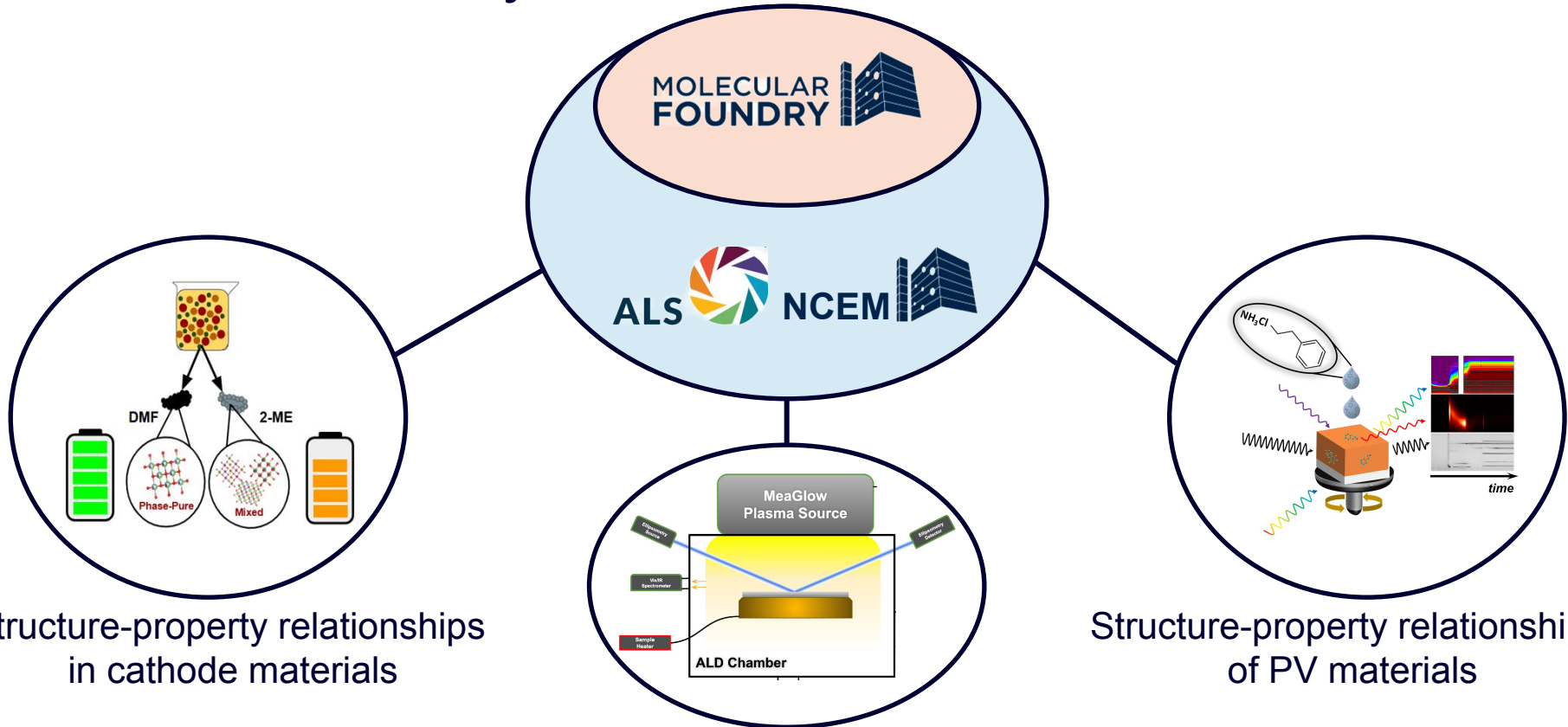
Berkeley Lab's NanoScale Research Center

- Glove boxes for synthesis in inert atm
- (Robotic) Thin film deposition tools
- Sol-gel powder synthesis
- In situ optoelectronic characterization; high-throughput XRD (all: Inorganic Nanostructures Facility)
- National Center for Electron Microscopy

Leveraging MF and ALS capabilities



Materials discovery and characterization

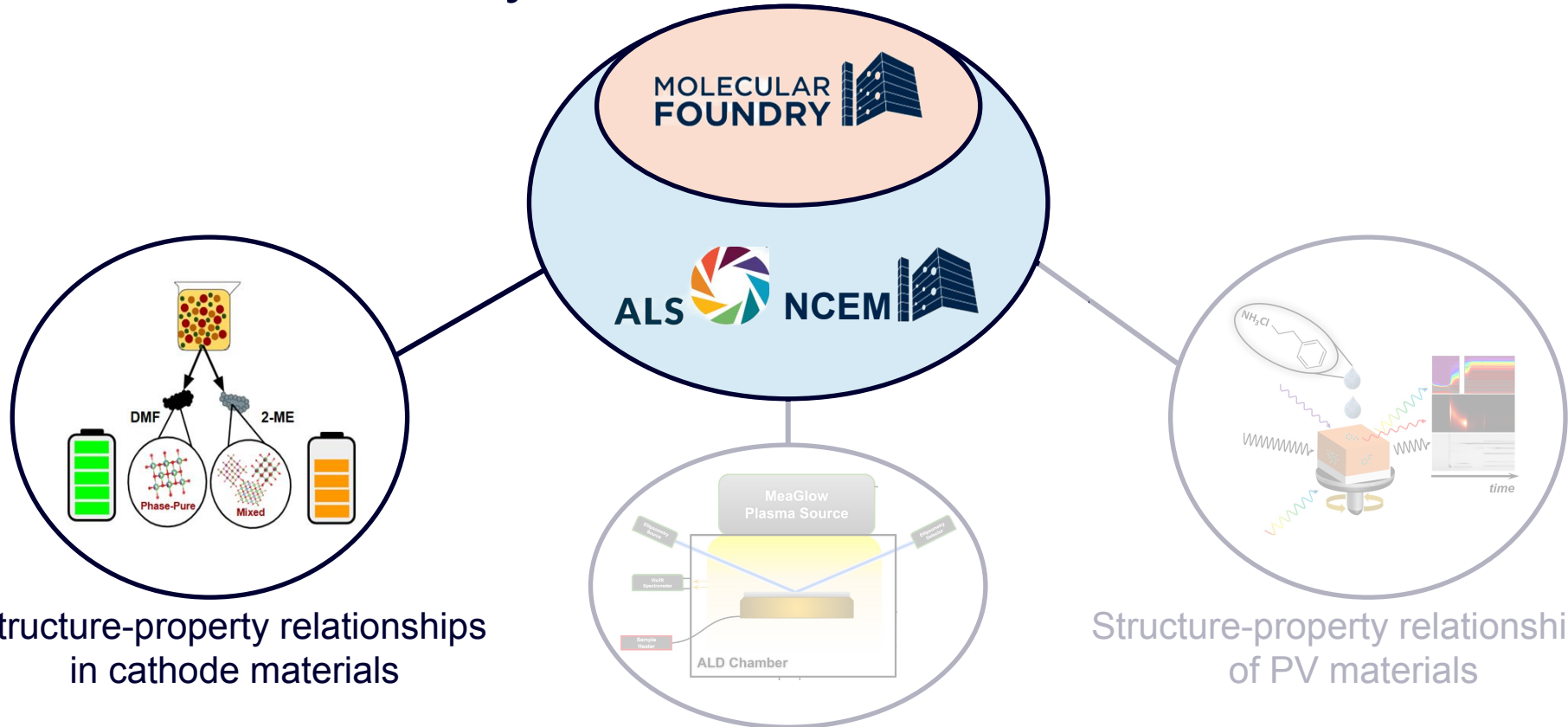


Structure-property relationships
in cathode materials

Closed loop, ML-driven,
robotic ALD

Structure-property relationships
of PV materials

Materials discovery and characterization



Structure-property relationships in cathode materials

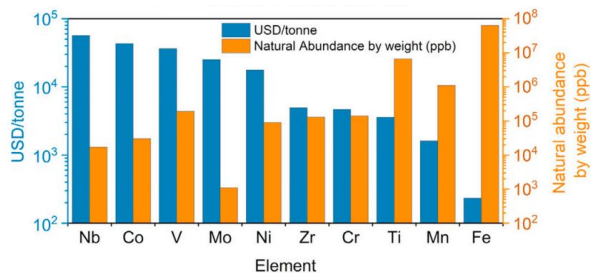
Closed loop, ML-driven, robotic ALD

Structure-property relationships of PV materials

Disordered rock salt enables replacement of Co and Ni in cathodes for Li-ion batteries

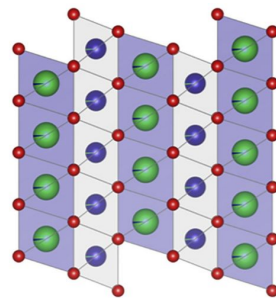
State-of-the-art layered cathodes for Li-ion batteries typically contain Co and/or Ni

□ expensive and non-abundant



H. Li et al. Joule 6, 53-91 (2022)

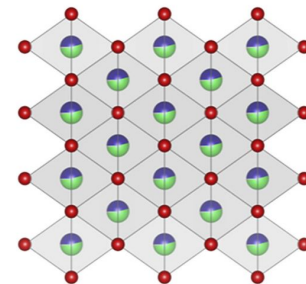
Replacing Co/Ni with other TMs in layered structures leads to poor Li-diffusion due to layer-contraction



Adapted from: S. W. D. Gourley et al. iScience 23 (9), 101505 (2020)



Disordered rock salt cathodes can tolerate other TMs



For efficient Li-diffusion, $\text{Li}_x\text{TM}_{2-x}\text{O}_2$ with $x > 1.1$ needed, here $\text{Li}_{1.2}\text{Mn}_{0.4}\text{Ti}_{0.4}\text{O}_2$

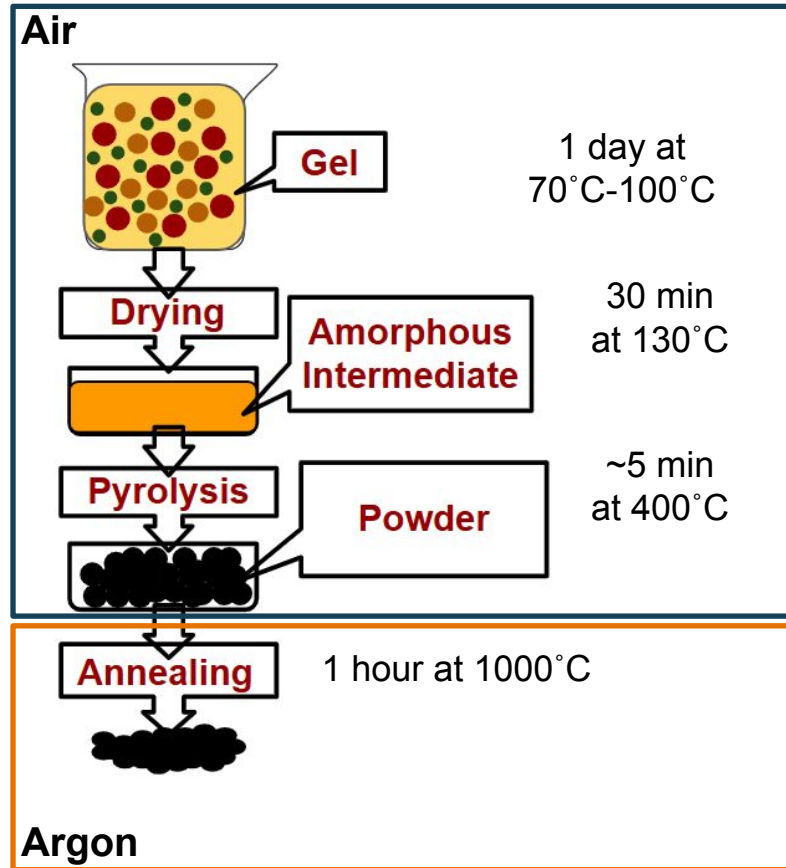
Major challenges for solid state synthesis of $\text{Li}_{1.2}\text{Mn}_{0.4}\text{Ti}_{0.4}\text{O}_2$ (DRX):

- Poor control over particle morphology and size
- High annealing temperatures and intense mechanical mixing/milling needed to achieve DRX-phase

T. N. L. Doan, et al., Front. Energy Res. 2 (2014)

□ Sol gel synthesis can potentially overcome these challenges

Sol-Gel Synthesis of LMTO-DRX



Goal:

Obtain **phase pure** & small-grained **DRX-material**

Solution engineering

Solvents:

Water & 2-Methoxyethanol
DMF (+ Water)
Ethanol (+ Water)
Water & Ethylene Glycol
Methanol (+Water)

Metal-Precursors:

Lithium Acetate / Li Hydroxide / Li Nitrate / ...
Manganese(II) Acetate / Manganese(III) Acetate / ...
Titanium Isopropoxide

Acidic Agents:

Citric Acid
Nitric Acid
Acetic Acid

Composition:

Li-to-TM ratio
Mn/Ti-ratio

High throughput parameter screening via automated synthesis & XRD

Spinbot One



Automatic solution engineering & thin film deposition:

- Precursor solution mixing
- Spin-coating
- Annealing
- Optoelectronic in-line characterization

High-Throughput XRD

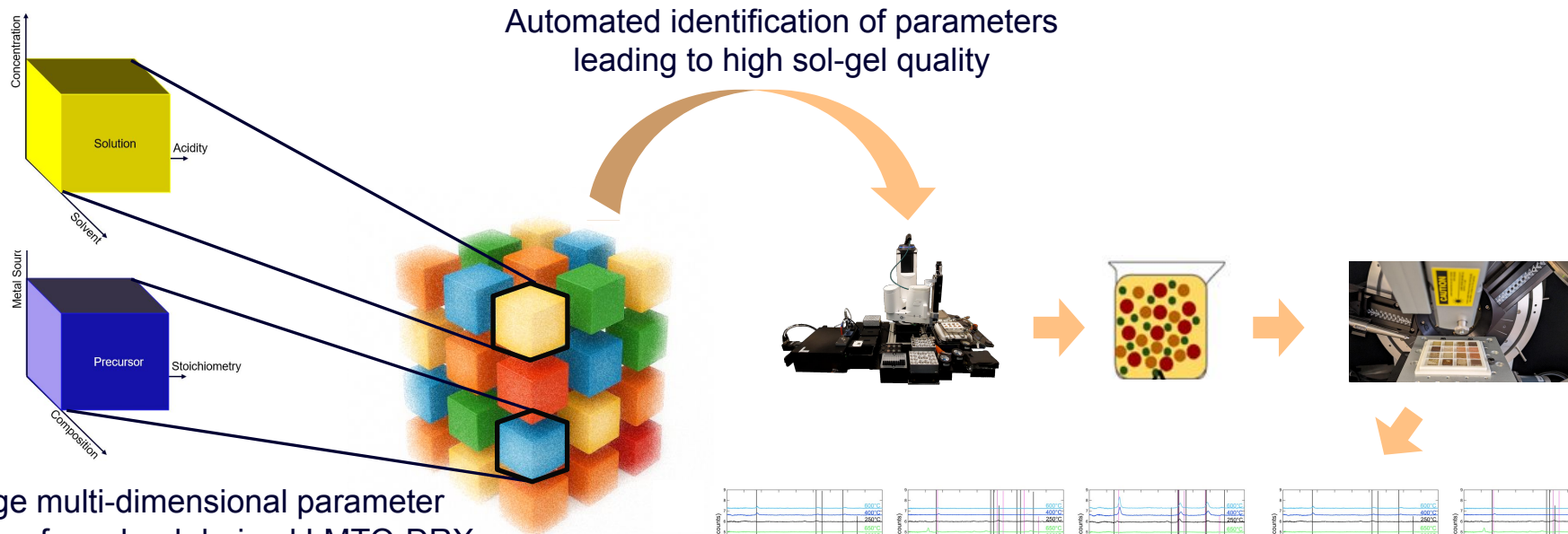


Batch characterization:

- 16 samples per batch
- Automated alignment & measurement
- Automated data integration and visualization

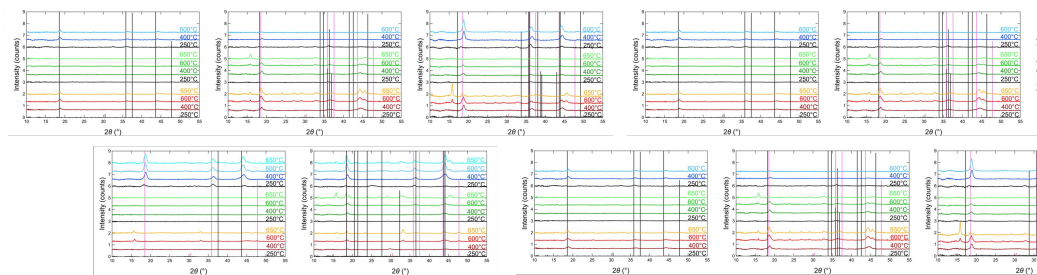


High throughput parameter screening via automated synthesis & XRD

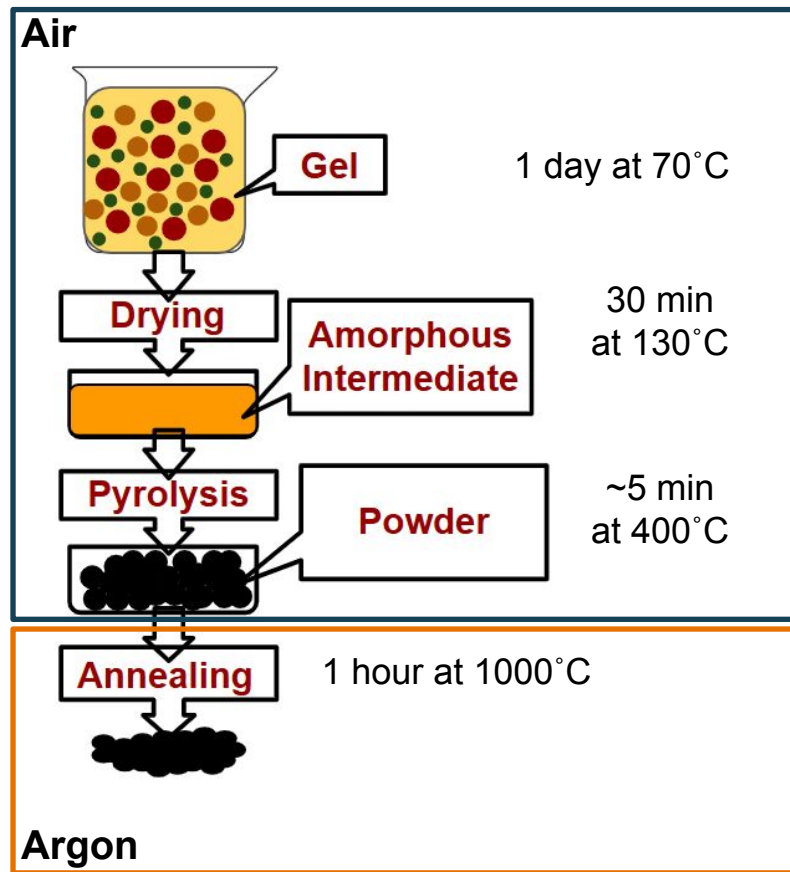


Large multi-dimensional parameter space for sol-gel derived LMTO-DRX:

- Solution
- Precursor chemistry
- Hydrolysis
- Gelification
- Pyrolysis
- ...



Choice of solvent is the most influential parameter for DRX-phase purity



Engineering approaches

Solvents:

Water & 2-Methoxyethanol

DMF (+ Water)

Ethanol (+ Water)

Water & Ethylene Glycol

Metal-Precursors:

Lithium Acetate / Li Hydroxide / Li Nitrate

Manganese(II) Acetate / Manganese(III) Acetate

Titanium Isopropoxide

Acidic Agents:

Citric Acid

Nitric Acid

Acetic Acid

Compositional Engineering:

Li-to-TM ratio

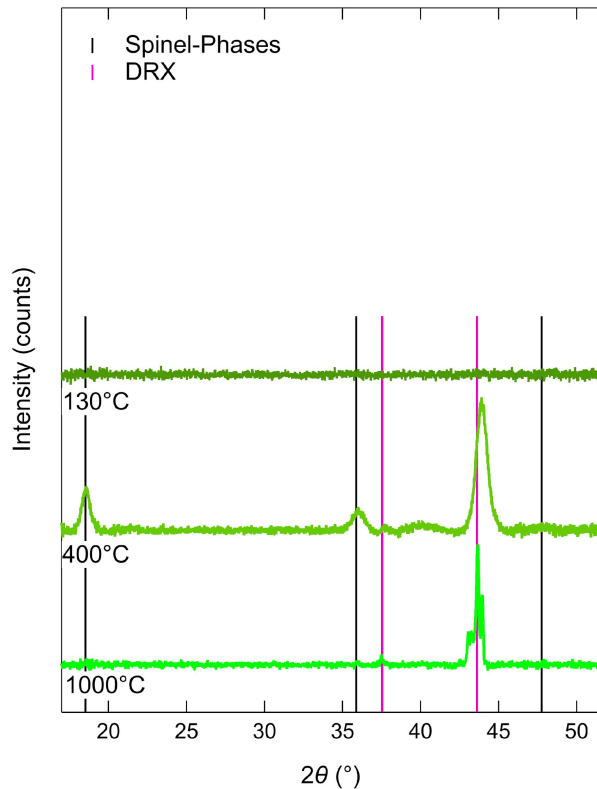
Mn/Ti-ratio

pH-control

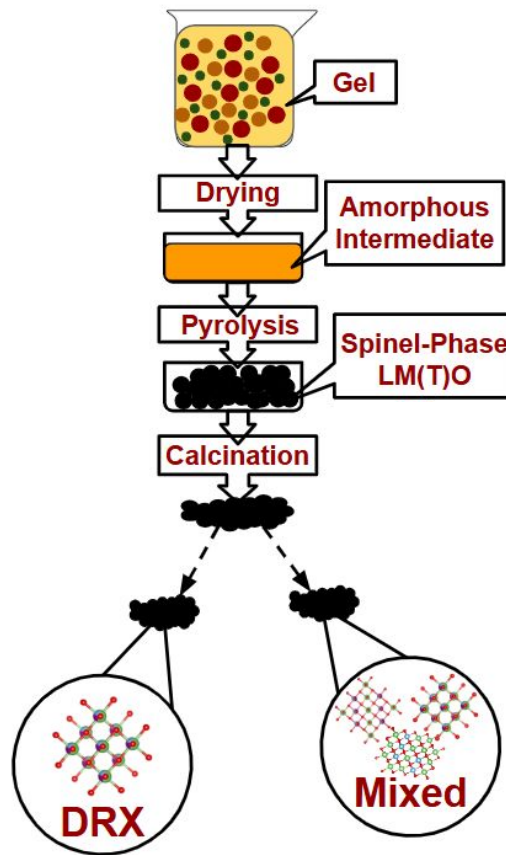
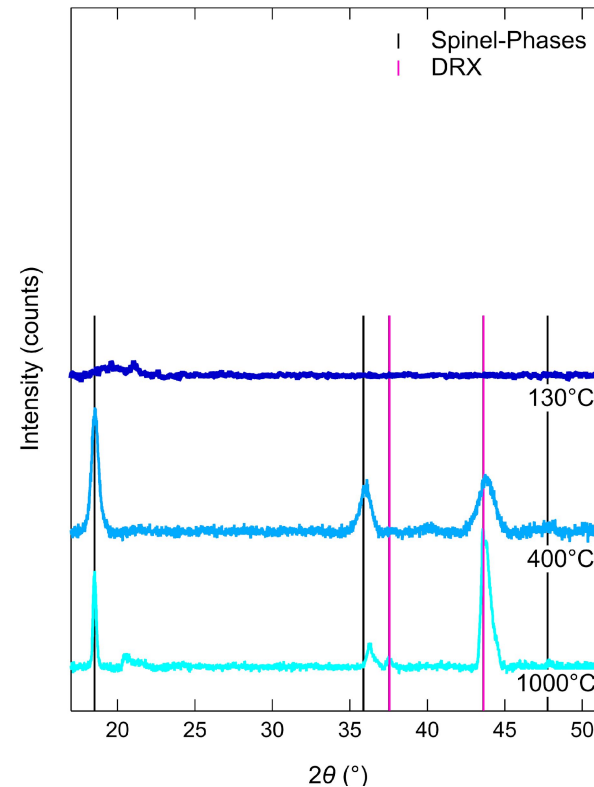


Choice of solvent is the most influential parameter for DRX-phase purity

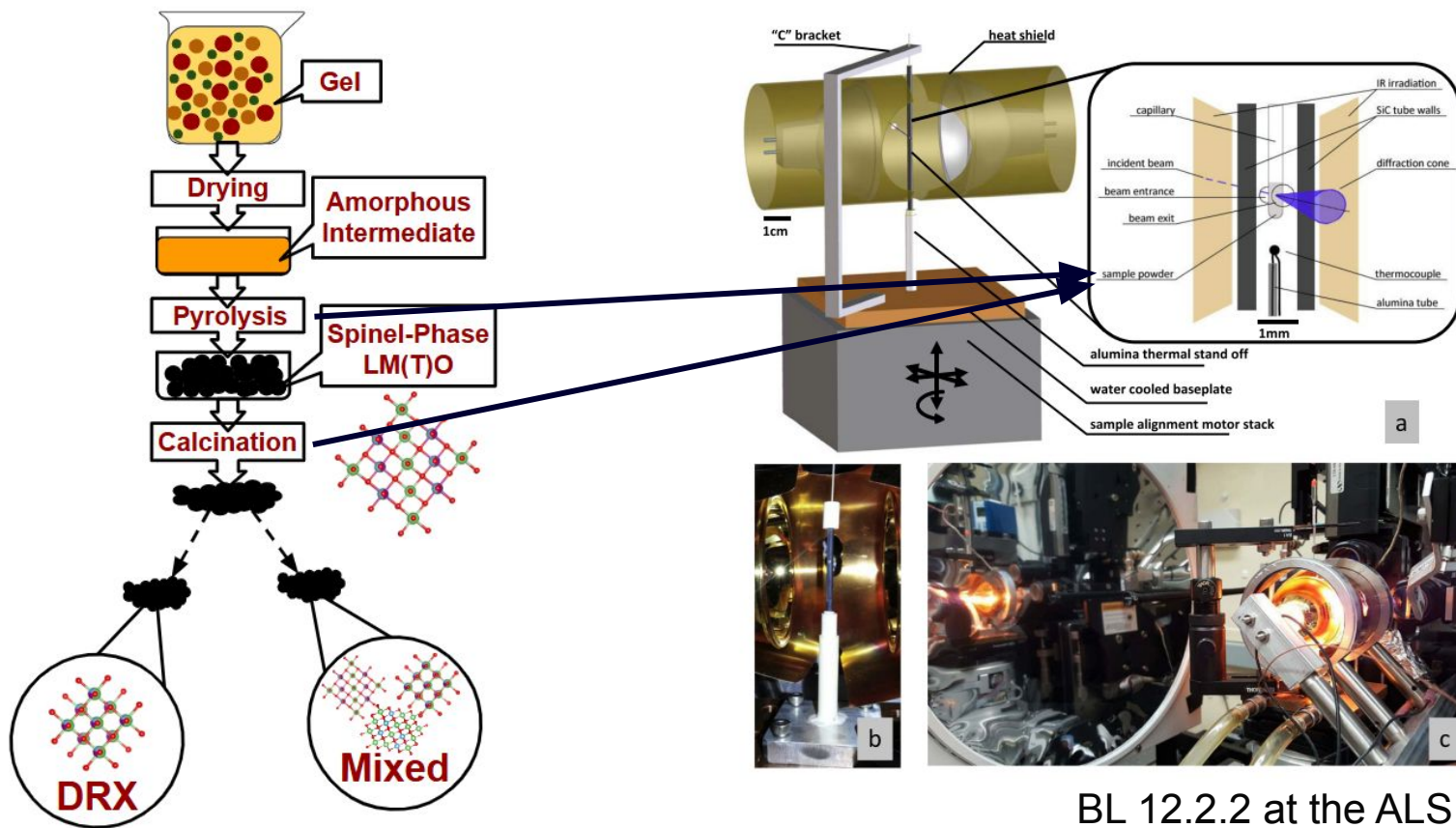
DMF



2-ME

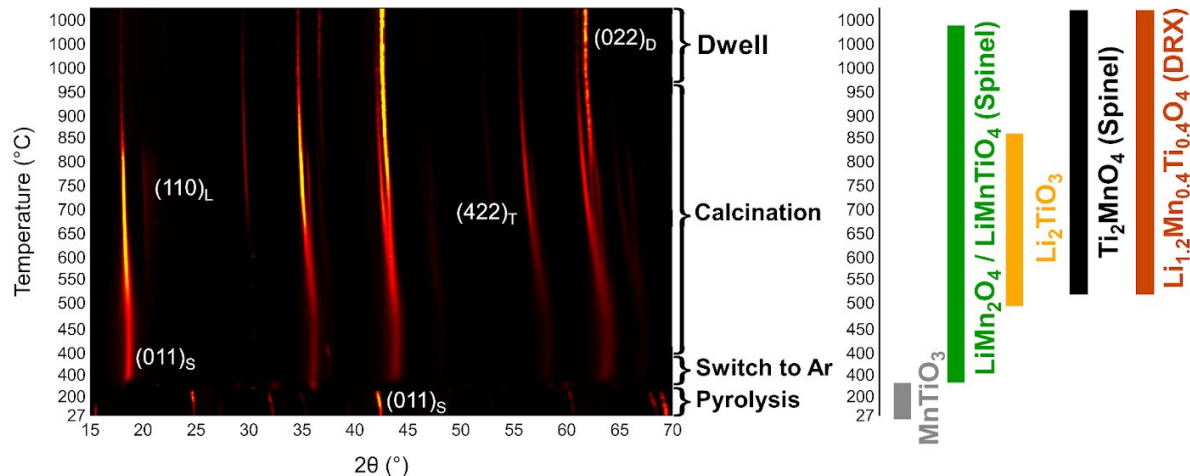


In situ pXRD during pyrolysis and calcination reveals driving force for impurity-formation



BL 12.2.2 at the ALS

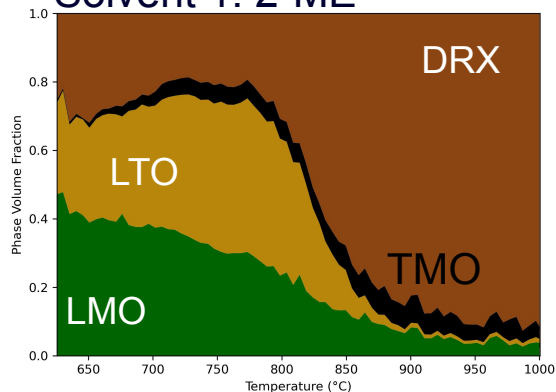
In situ pXRD during pyrolysis and calcination reveals driving force for impurity-formation



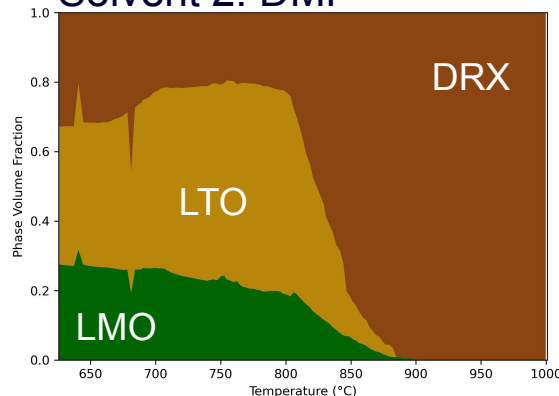
2-ME + Water as solvent:

- Main DRX-formation window between 775°C and 860°C
- Intermediate phase formation around 400°C to 500°C:
 - LiMnO₂ (Mn-rich)
 - Li₂TiO₃ (Ti-rich)
 - Ti₂MnO₄ (Ti-rich)

Solvent 1: 2-ME



Solvent 2: DMF



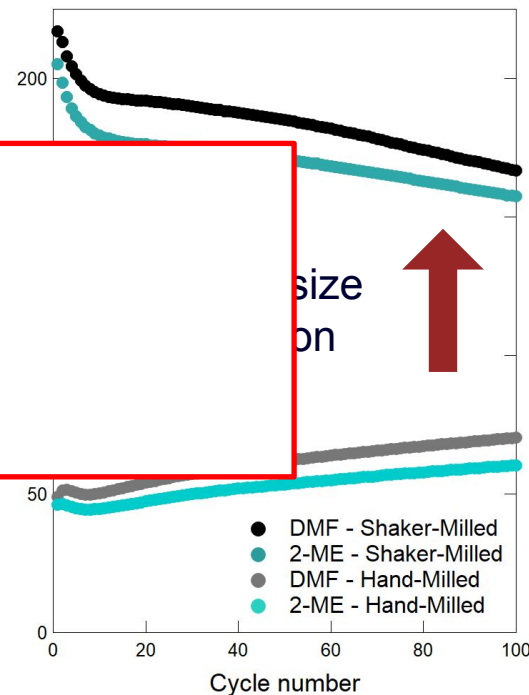
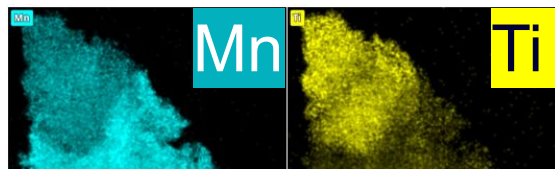
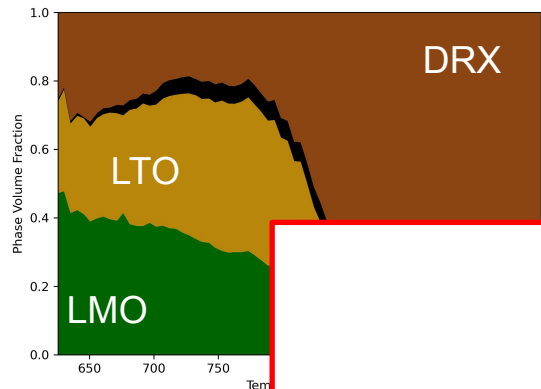
DMF + Water as solvent:

- Main DRX-formation window between 775°C and 860°C
- No Ti₂MnO₄ formation
→ phase purity at 900°C

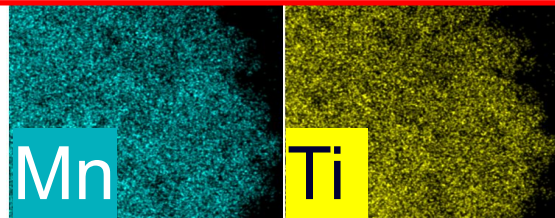
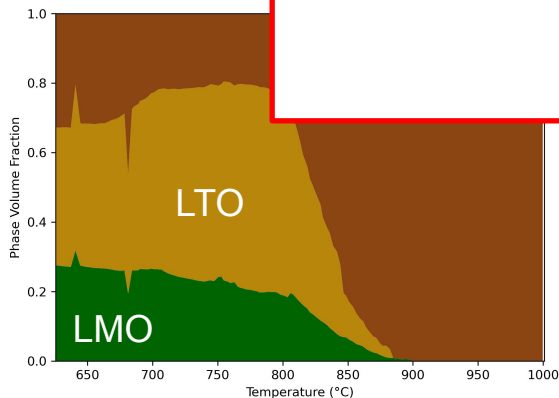
T. Kodalle et al., Nano Letters 25(30), 2025.

Choice of solvent determines phase purity & cell performance

Solvent 1: 2-ME

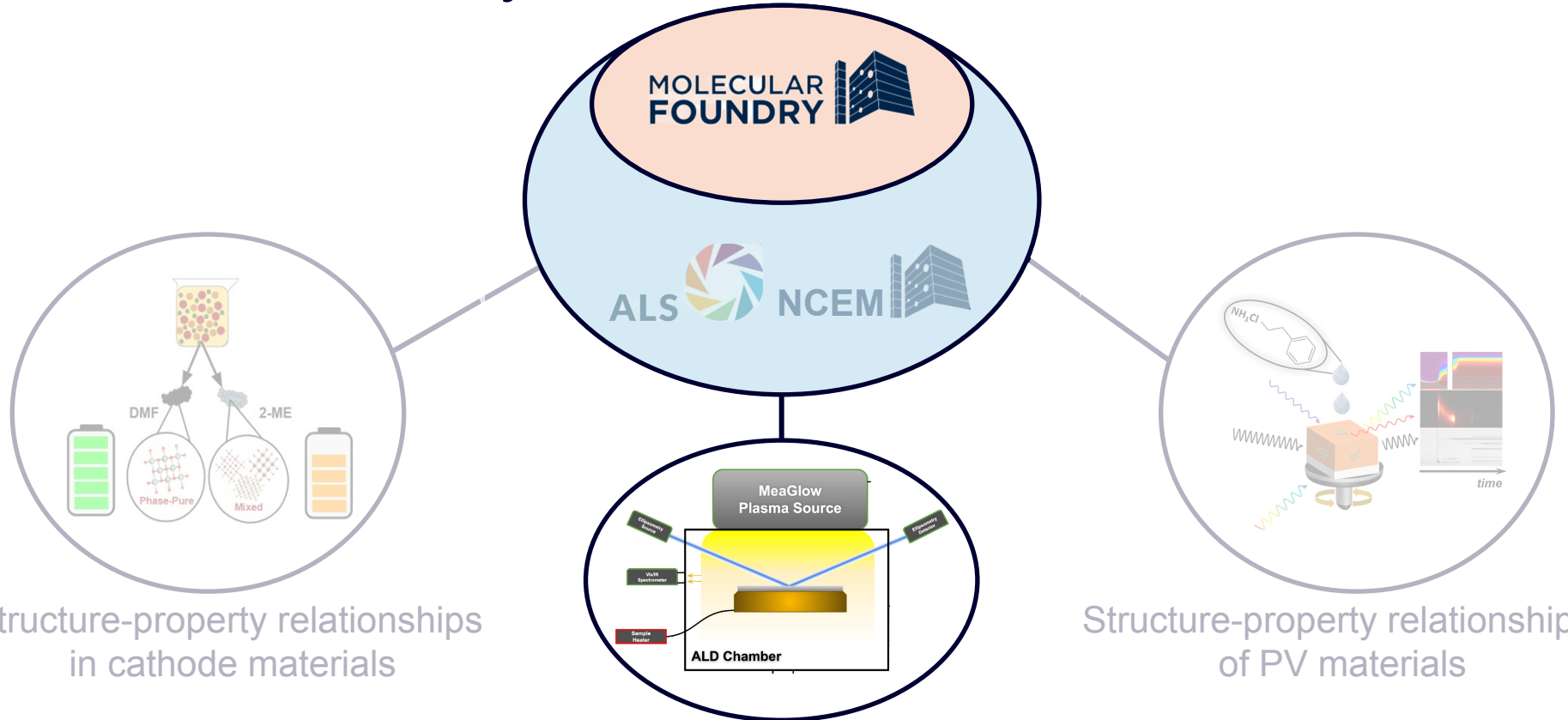


Solvent 2: DMF



Next Step:
Limit particle growth via solution
and process engineering

Materials discovery and characterization

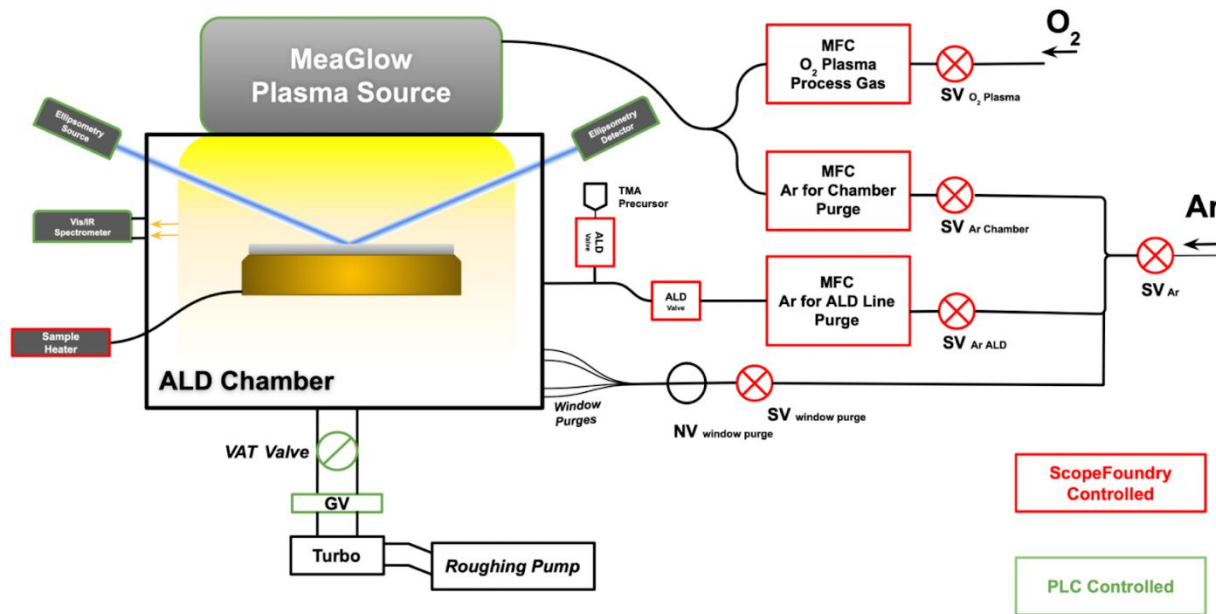


Structure-property relationships
in cathode materials

Closed loop, ML-driven,
robotic ALD

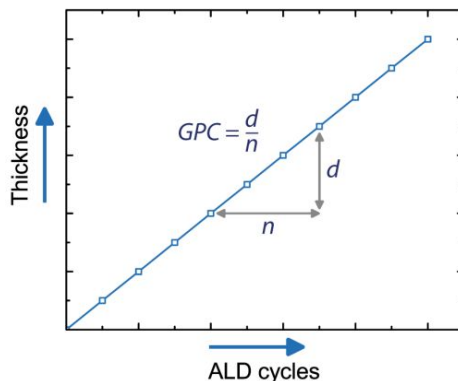
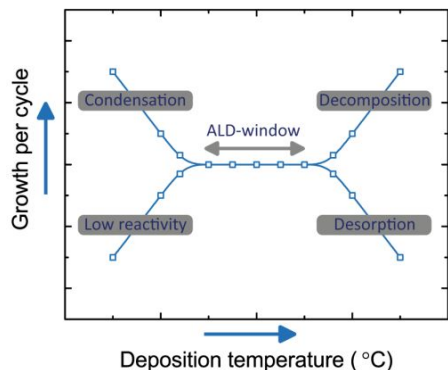
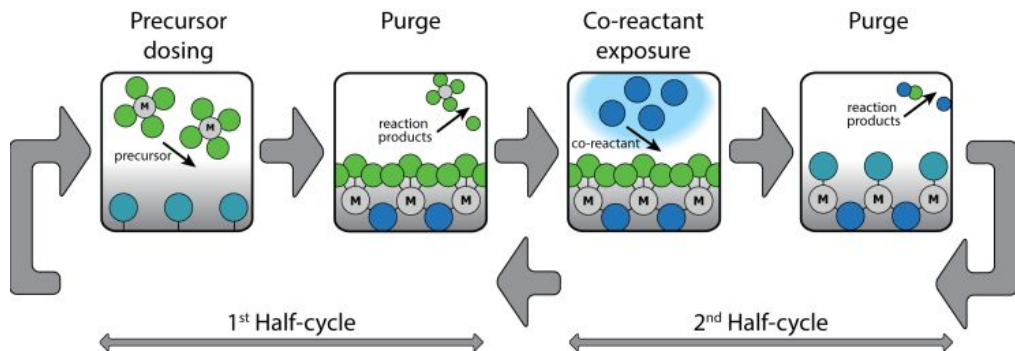
Structure-property relationships
of PV materials

Robotic PE-ALD tool for fast process optimization



- In-house constructed ALD-Tool with integrated software control system: “ALDBot”
- Test system: ALD-TiO₂ for microelectronics/catalysis
- **Main goal: Closed loop parameter space exploration and optimization**

ML-assisted exploration of the ALD parameter space using Gaussian Processing



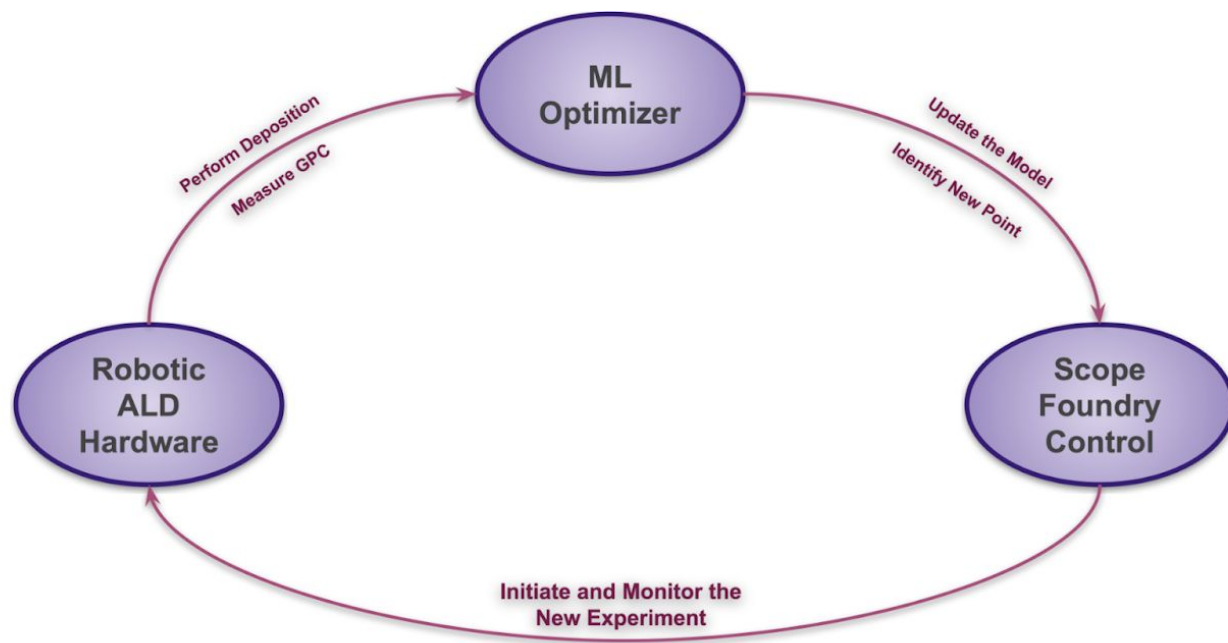
20-dimensional parameter space for ALD and plasma conditions:

```

"params": {
  "process_pressure": 10,
  "precursor_dose_time": 1000,
  "ald_valves_delay": 10,
  "precursor_purge_time": 2000,
  "H2_plasma_flow_rate": 75,
  "Ar_process_flow_rate": 50,
  "ALD_purge_flow_rate": 5,
  "ALD_prep_time": 2000,
  "ALD_purge_time": 2000,
  "plasma_pressure": 60,
  "N2_plasma_flow_rate": 0,
  "Ar_plasma_flow_rate": 0,
  "ALD_purge_plasma_flow_rate": 0,
  "RF_power_setpoint": 100,
  "plasma_duration": 2000,
  "LC_preset": 50,
  "TC_preset": 30,
  "plasma_prep_time": 3000,
  "plasma_purge_time": 500,
  "Number_of_ALD_cycles": 25
},
    
```

+ Substrate and precursor temperature

Robotic PE-ALD tool for fast process optimization

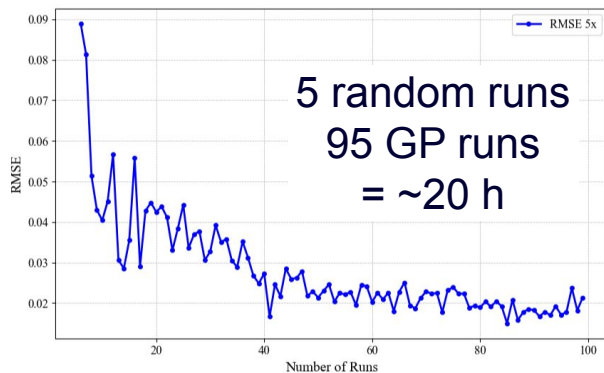


- In-house constructed ALD-Tool with integrated software control system: “ALDBot”
- Test system: ALD-TiO₂ for microelectronics
- **Main goal: Closed loop parameter space exploration and optimization**
- **Secondary Goal: Finding the “ALD-Window” for TiO₂**

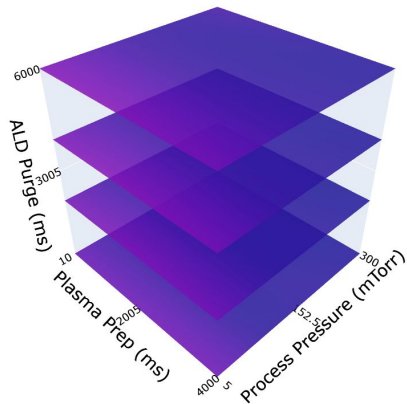
ML-assisted exploration of the ALD parameter space using Gaussian Processing

Demonstration: Explore 4D parameter space

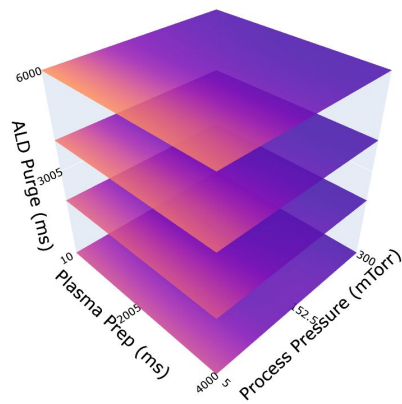
- Precursor Dose Time
- ALD Purge Time
- Plasma Preparation Time
- Process Pressure



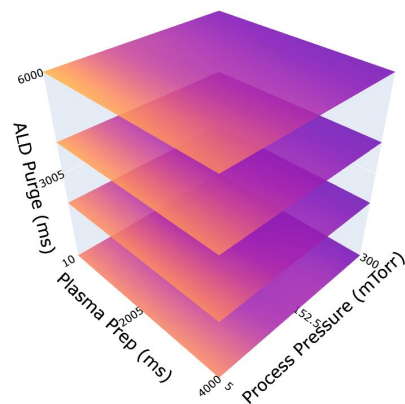
Dose Time = 1 s



Dose Time = 3 s



Dose Time = 5 s



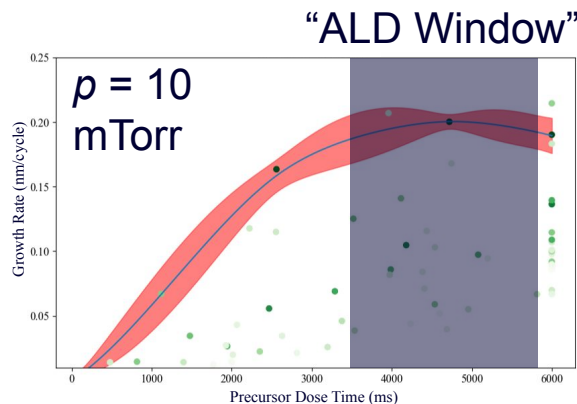
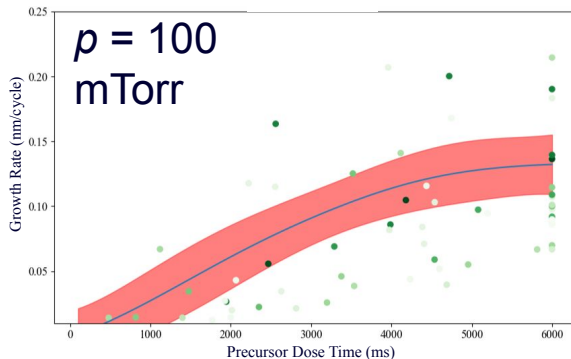
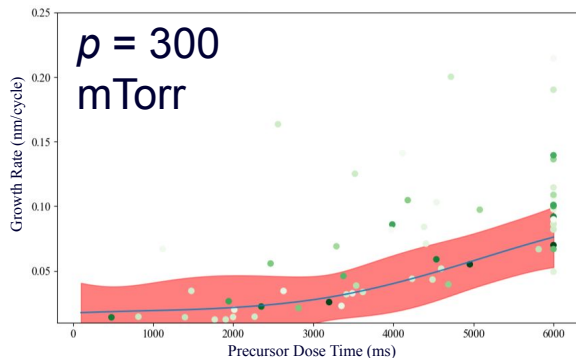
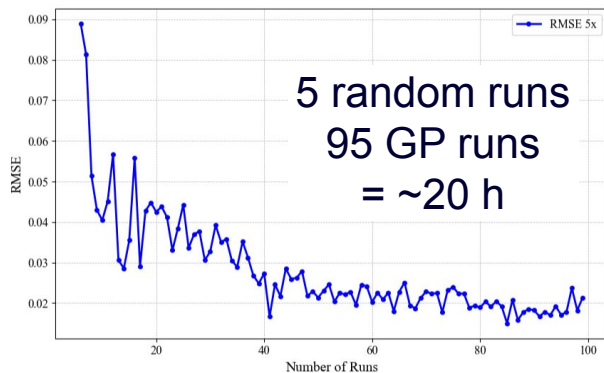
Growth Rate (nm)



ML-assisted exploration of the ALD parameter space using Gaussian Processing

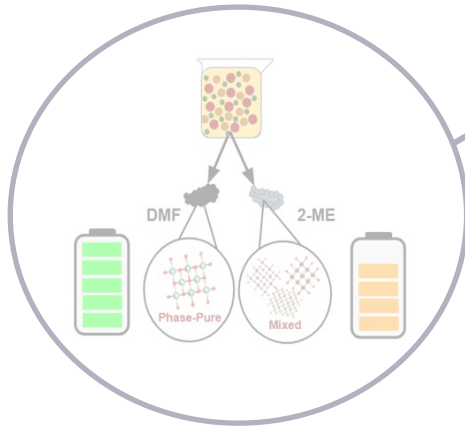
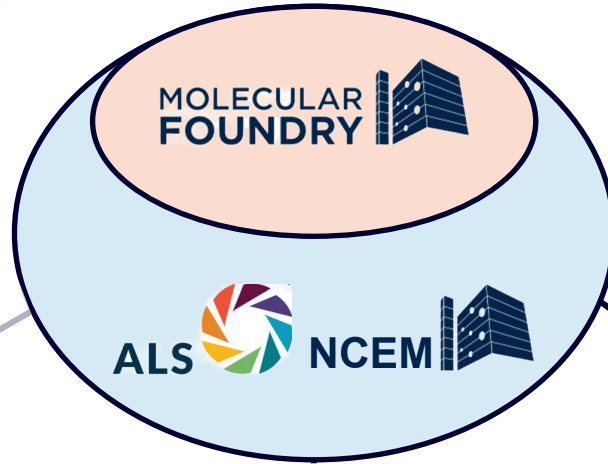
Demonstration: Explore 4D parameter space

- Precursor Dose Time
- ALD Purge Time
- Plasma Preparation Time
- Process Pressure

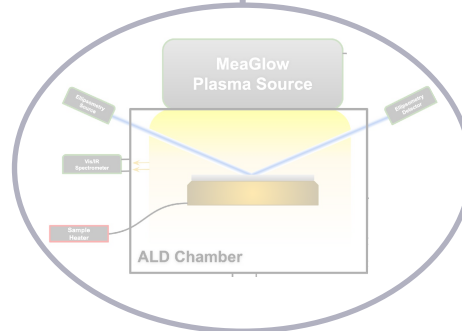


□ Working conditions for TiO_2 found within 1 day of experiments

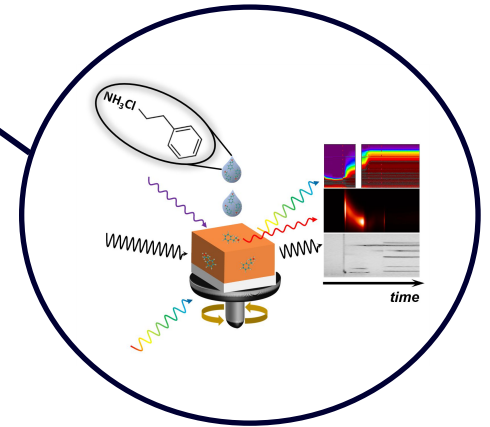
Materials discovery and characterization



Structure-property relationships
in cathode materials

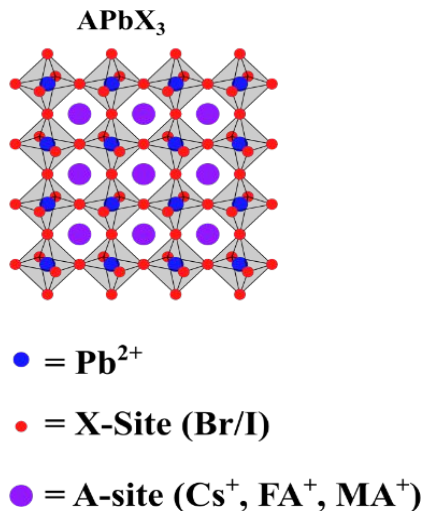


Closed loop, ML-driven,
robotic ALD

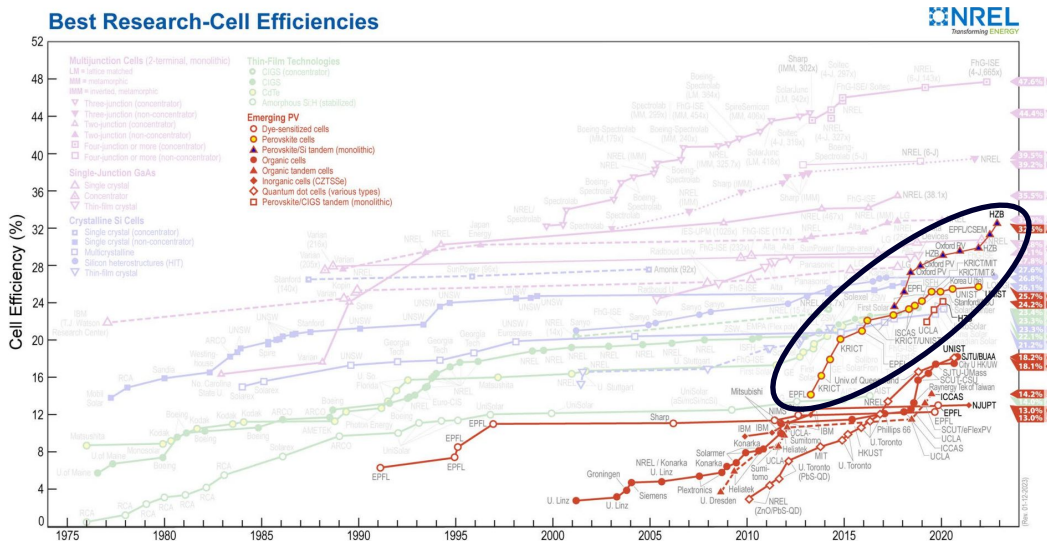


Structure-property relationships
of PV materials

Metal halide perovskites for photovoltaics



T. Kodalle et al., Adv. Ener. Mat. 13(33), 2201490, 2023



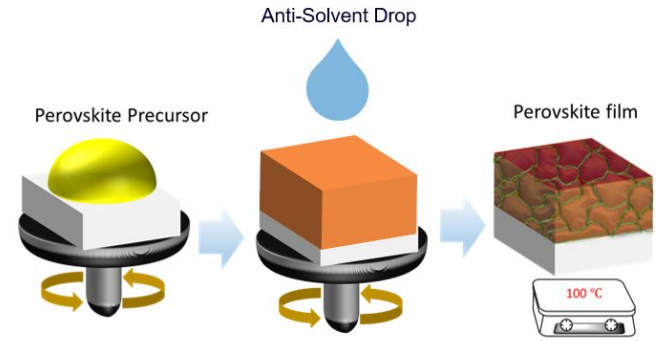
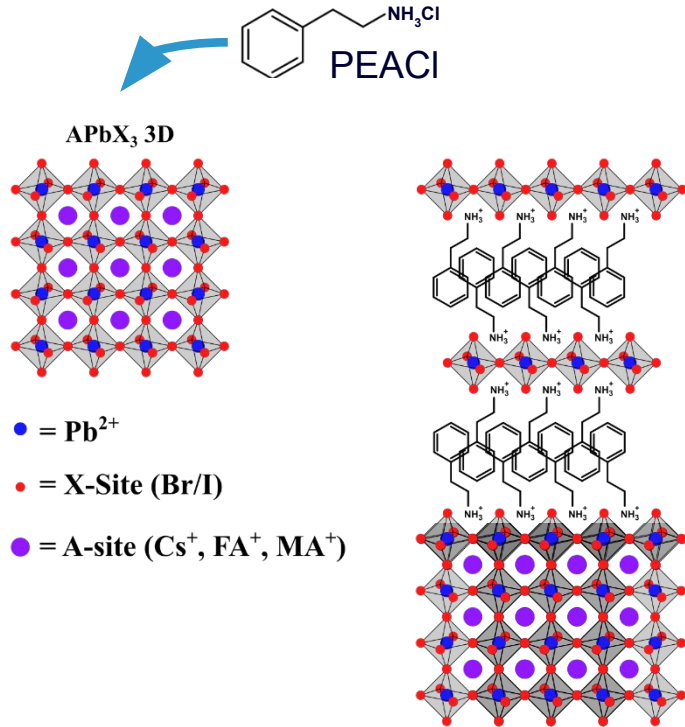
Main Issues:

- Toxicity
- Stability in ambient/humid environment

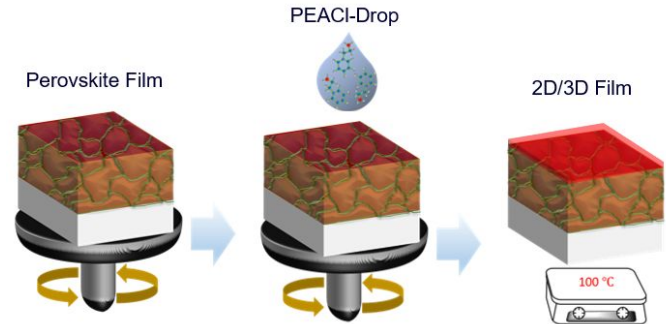


2D structures in halide perovskites for improved stability

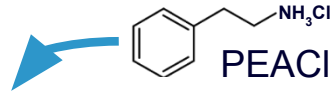
1. 3D Perovskite Deposition



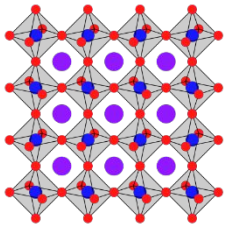
2. 2D Perovskite Formation



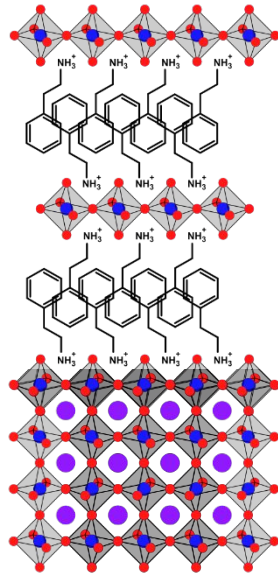
2D structures in halide perovskites for improved stability



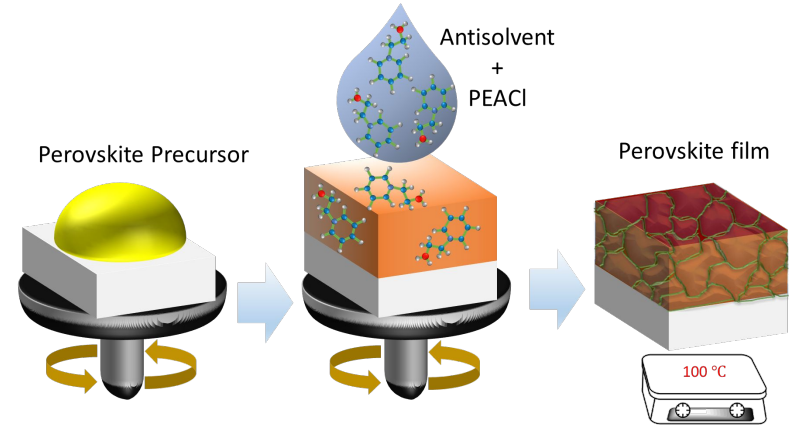
APbX₃ 3D



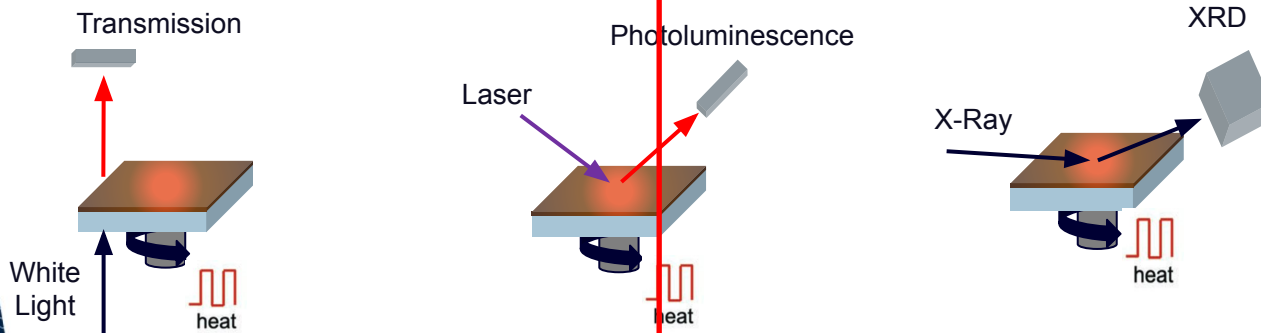
- = Pb²⁺
- = X-Site (Br/I)
- = A-site (Cs⁺, FA⁺, MA⁺)



1. Integrated 3D & 2D Perovskite Deposition



The MMSC – now a joint user program of the Foundry and ALS



Photoluminescence and transmission setups at the Molecular Foundry

Perovskite
Glovebox in the
Sutter-Fella Lab

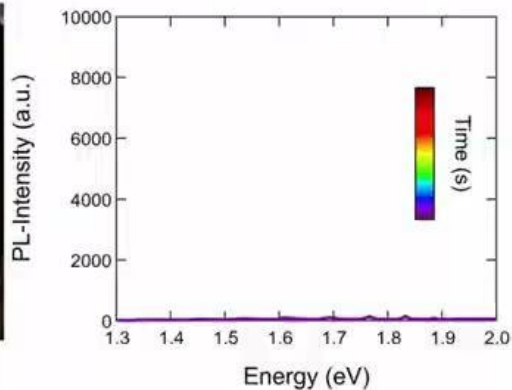


- Inert glove box atmosphere
- Same deposition conditions as in most device-oriented labs
- Time resolution around 0.1s

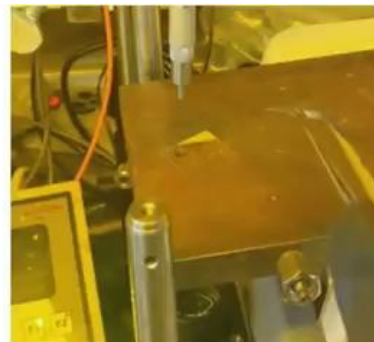
In Situ Photoluminescence



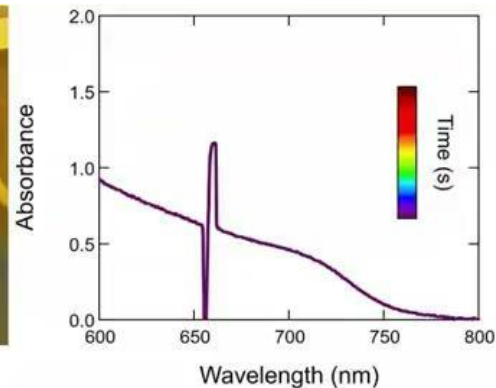
Spin-Coating



In Situ



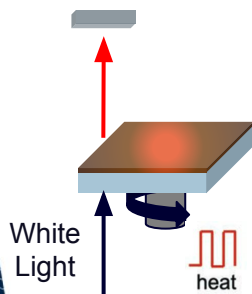
Annealing



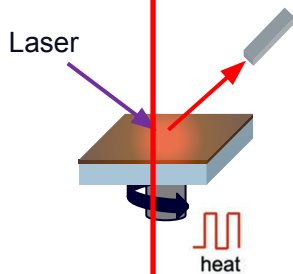
The MMSC-Program – a joint user program of the Foundry and ALS



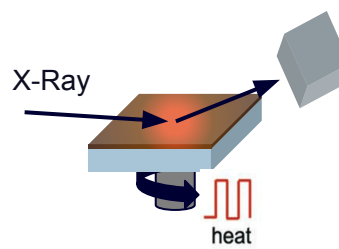
Transmission



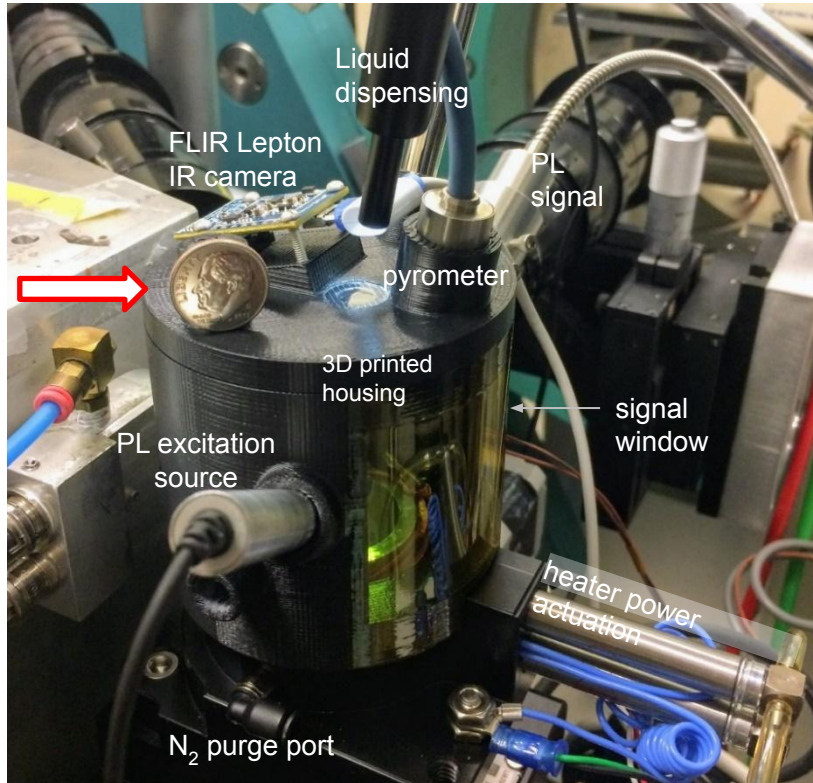
Photoluminescence



XRD

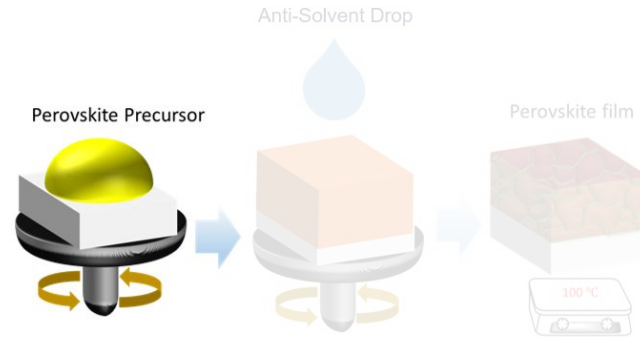
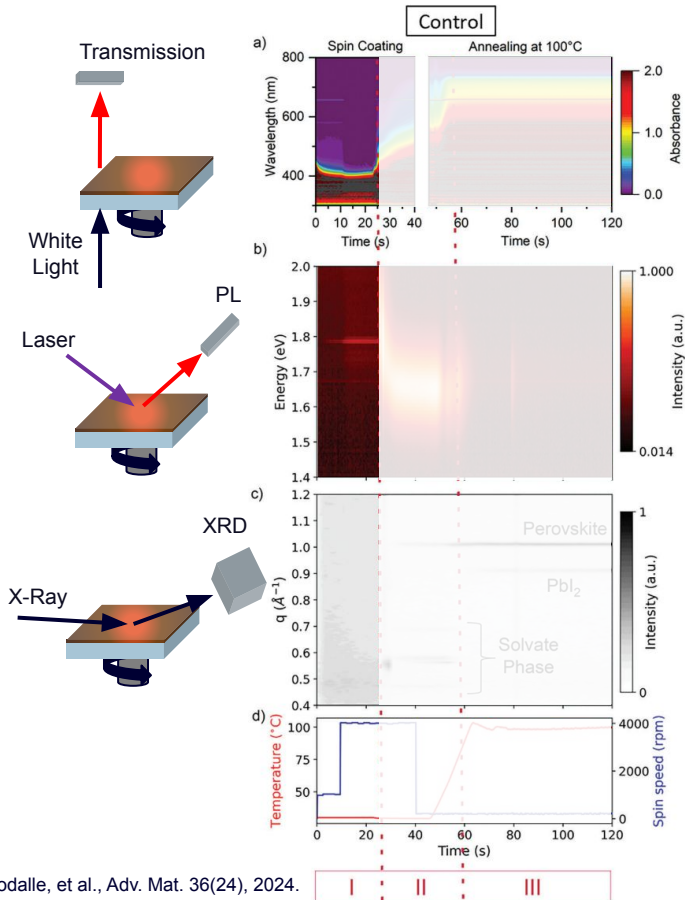


Multimodal in situ spin-coater at Beamline 12.3.2



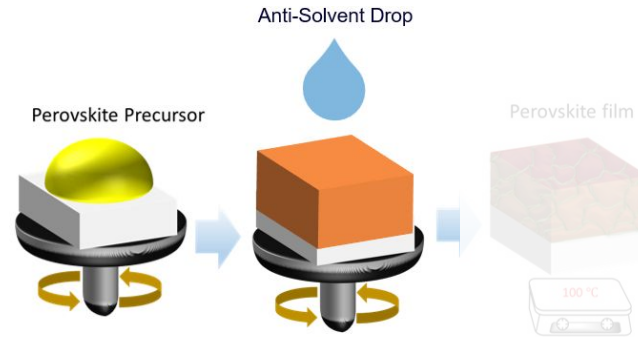
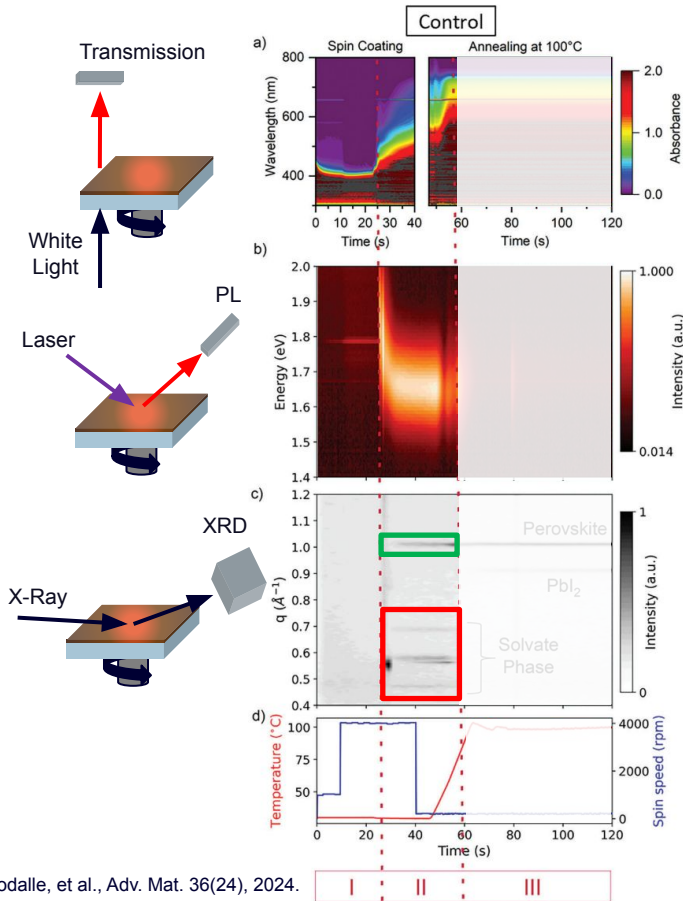
- Automated sequences of spin-coating, heating, and liquid dispensing in variable atmosphere
- Multimodal in situ photoluminescence and X-ray diffraction measurements
- Real time data acquisition (< 1s time resolution)
- Assembly at microdiffraction beamline allows for precise control of beam spot and incidence angle

Multimodal analysis of the perovskite growth: Reference case



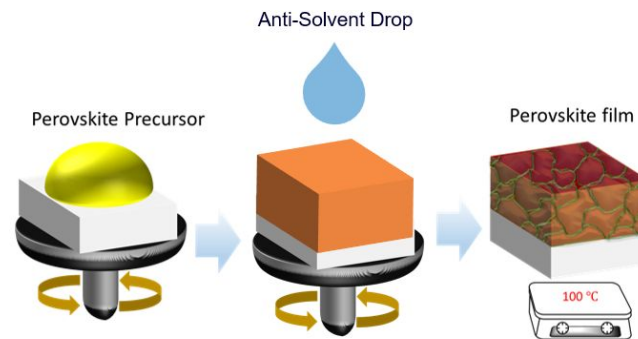
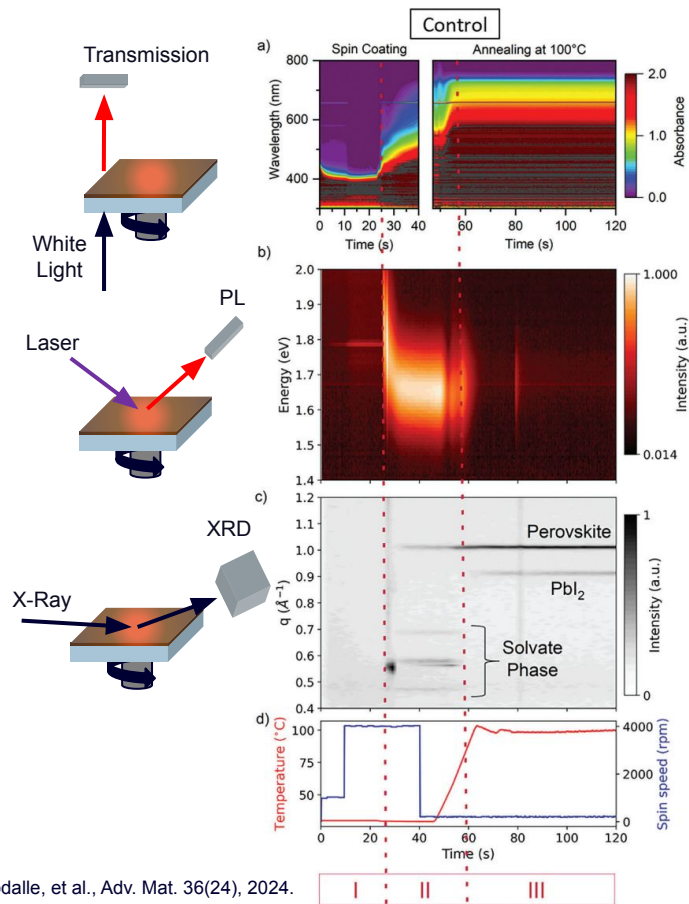
- Phase I (Spin-Coating): Wet film - No PL or WAXS signal

Multimodal analysis of the perovskite growth: Reference case



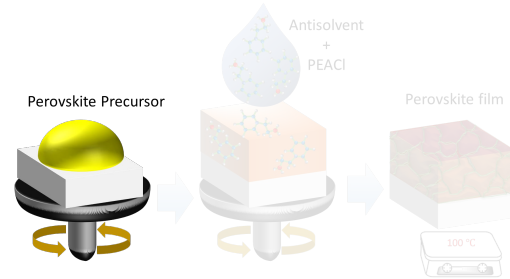
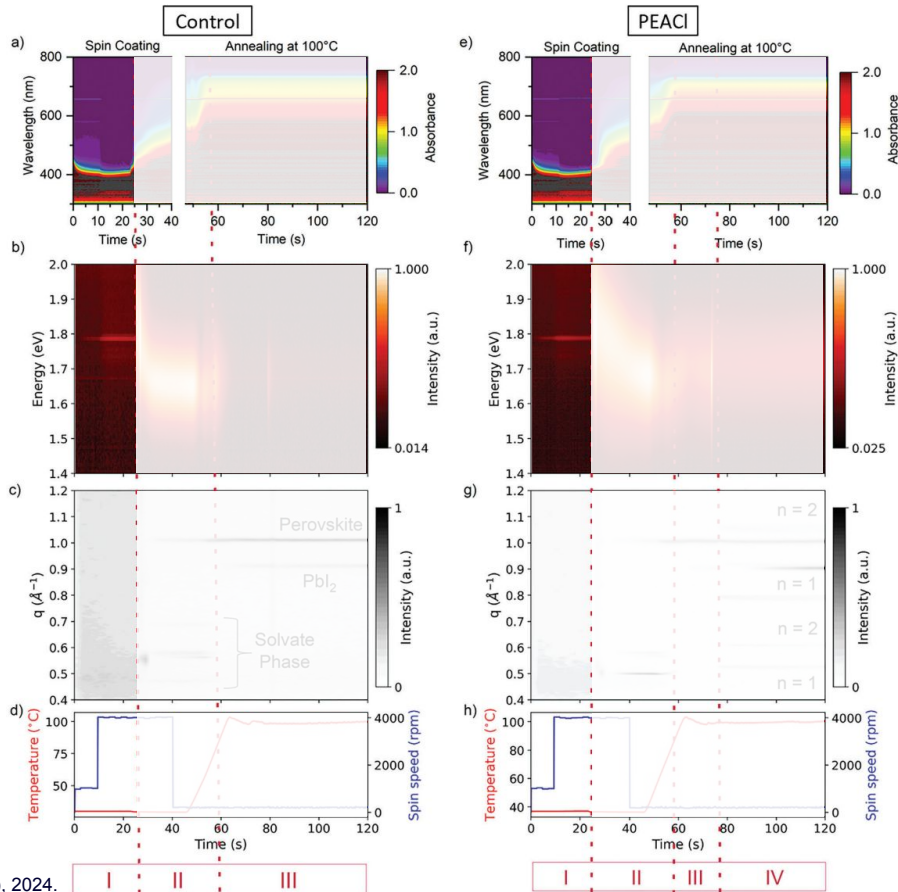
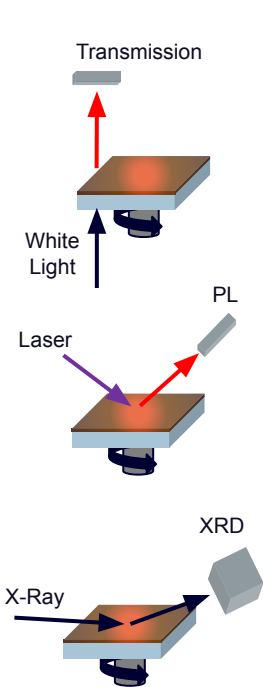
- Phase I (Spin-Coating): Wet film - No PL or WAXS signal
- Phase II (AS-Drop): Nucleation and growth of **intermediate** & **perovskite** phase

Multimodal analysis of the perovskite growth: Reference case



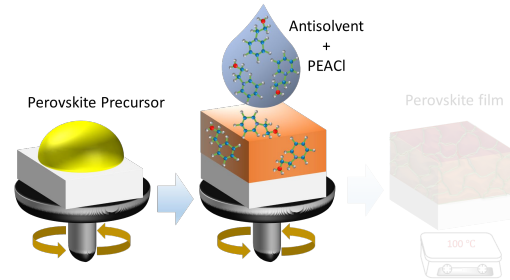
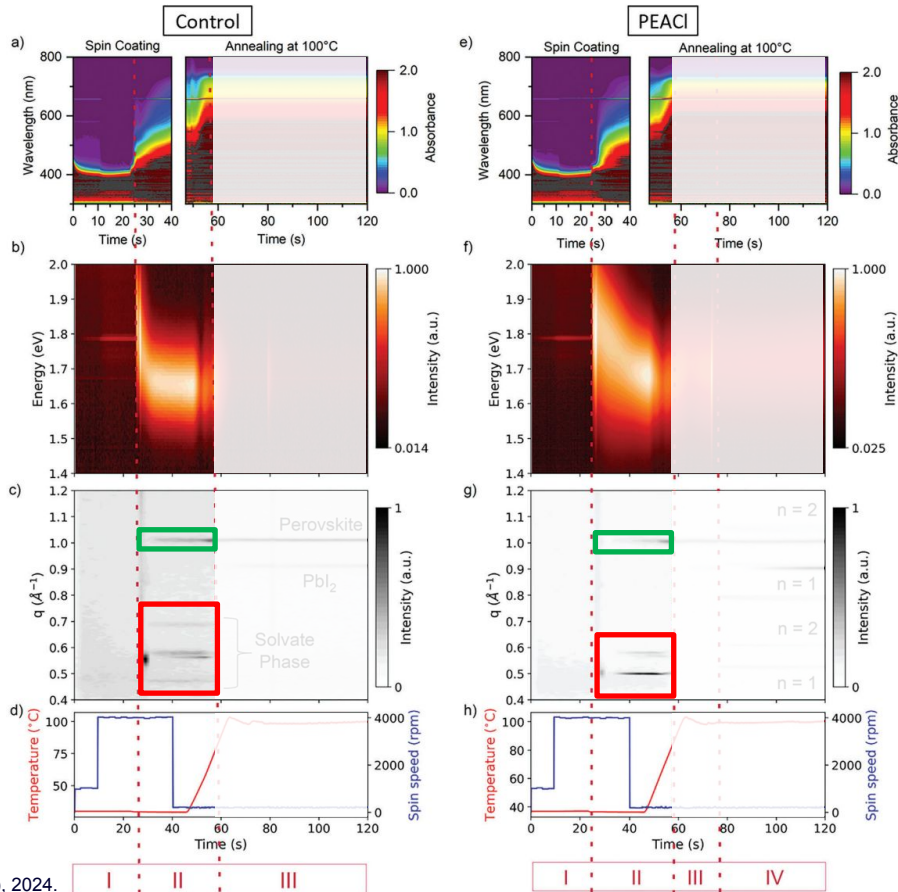
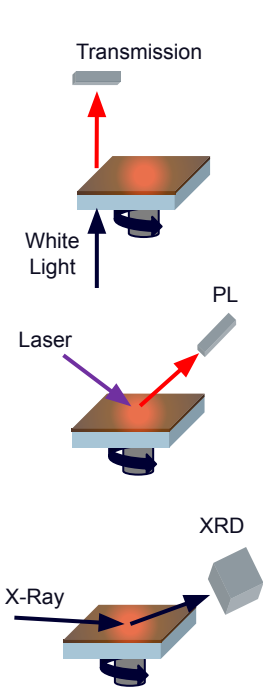
- Phase I (Spin-Coating): Wet film - No PL or WAXS signal
- Phase II (AS-Drop): Nucleation and growth of intermediate & perovskite phase
- Phase III (Annealing): Solvent-evaporation & crystal growth

Multimodal analysis of the perovskite growth: PEACl case



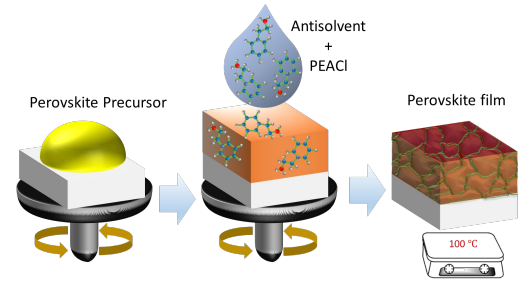
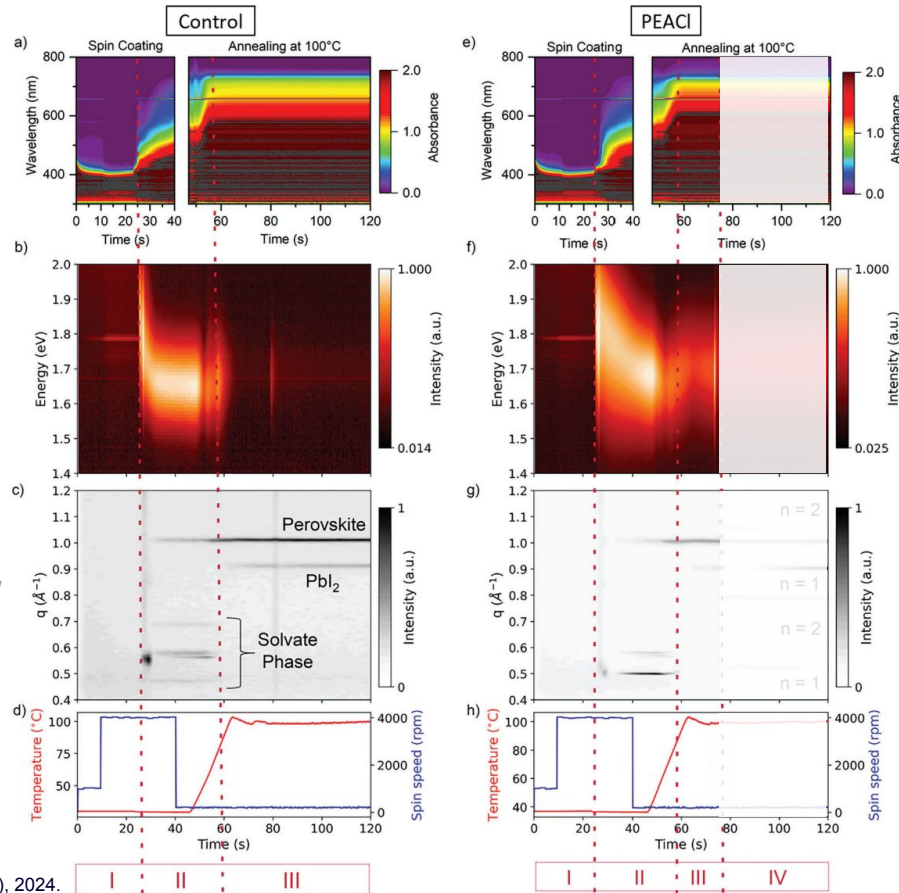
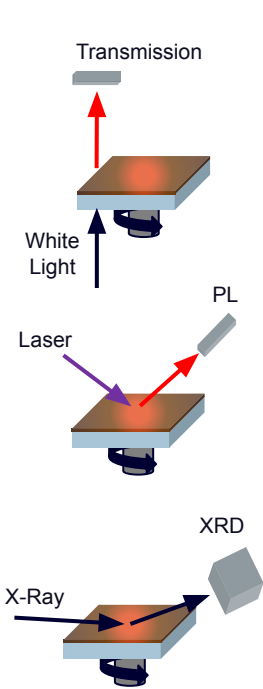
• Phase I (Spin-Coating): Wet film

Multimodal analysis of the perovskite growth: PEACl case



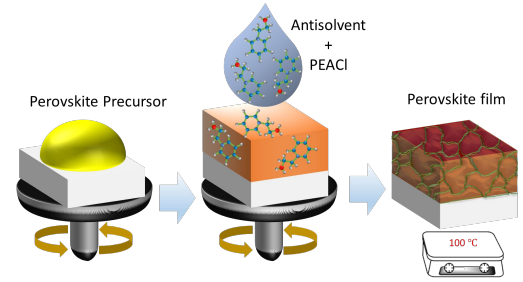
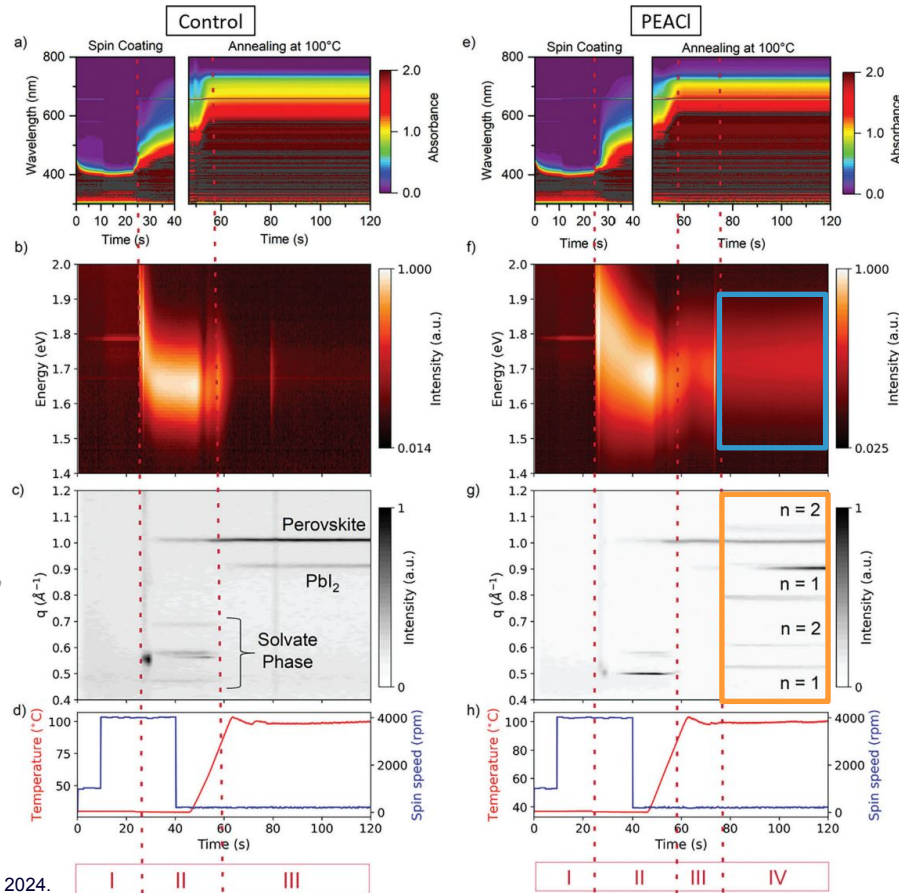
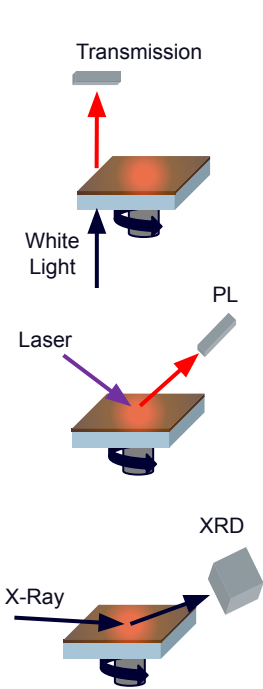
- Phase I (Spin-Coating): Wet film
- Phase II (PEACl-Drop): **Slower nucleation of pvsk-phase, altered intermediate phase**

Multimodal analysis of the perovskite growth: PEACl case



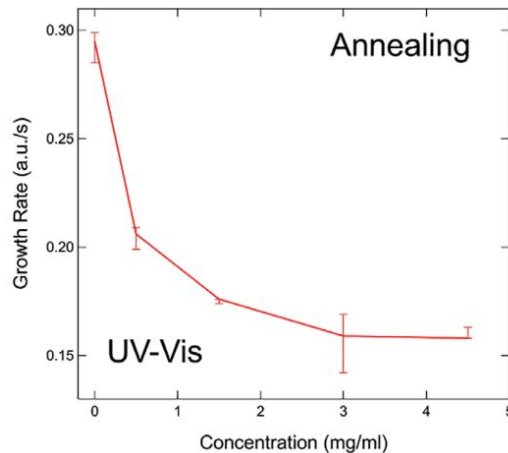
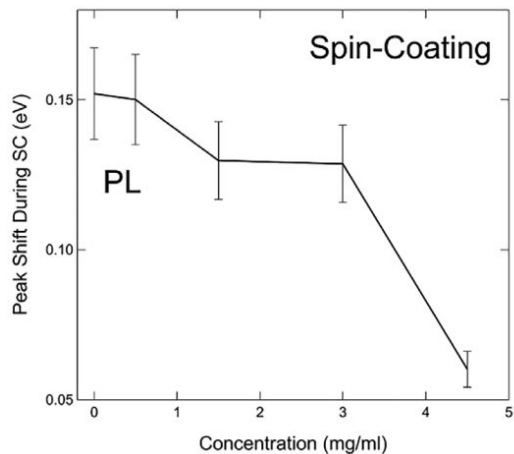
- Phase I (Spin-Coating): Wet film
- Phase II (PEACl-Drop): Slower nucleation of pvsk-phase, altered intermediate phase
- Phase III (Annealing): Solvent-evaporation & crystal growth

Multimodal analysis of the perovskite growth: PEACl case

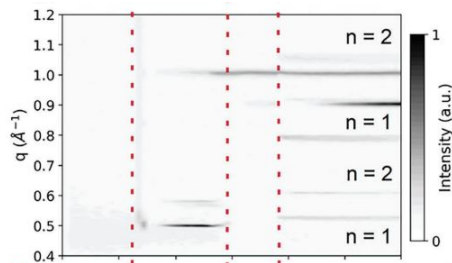
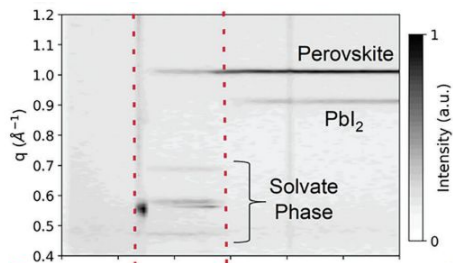


- Phase I (Spin-Coating): Wet film
- Phase II (PEACl-Drop): Slower nucleation of pvsk-phase, altered intermediate phase
- Phase III (Annealing): Solvent-evaporation & crystal growth
- Phase IV: Intercalation of PEACl, improved crystal quality

Varying PEACl-Concentration confirms improved growth

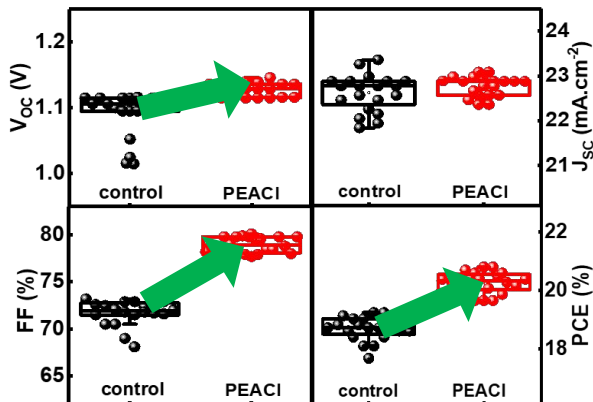
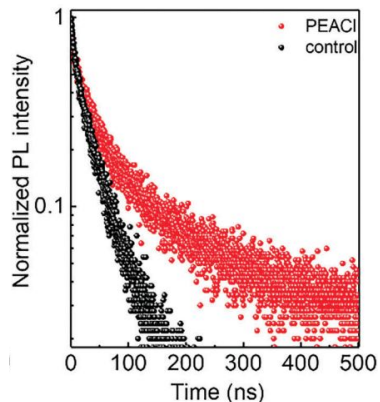
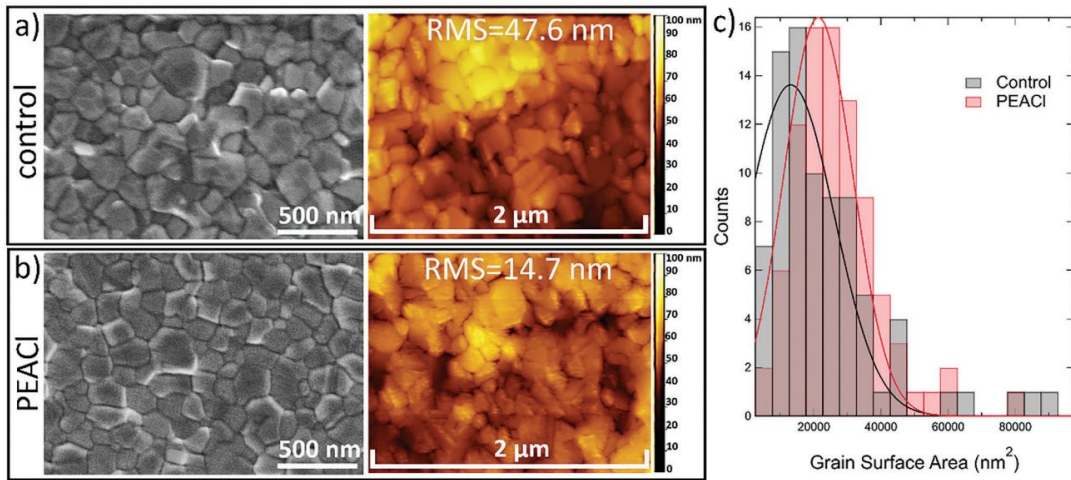


- PEACl slows down perovskite nucleation and crystal growth (UV-Vis & PL)



- Intermediate solvate phases form in both cases – but incorporates Cl in PEACl case (GIWAXS)

Correlation with ex situ characterization



- SEM & KPFM: Slower nucleation leads to growth of larger grains, smoother surface



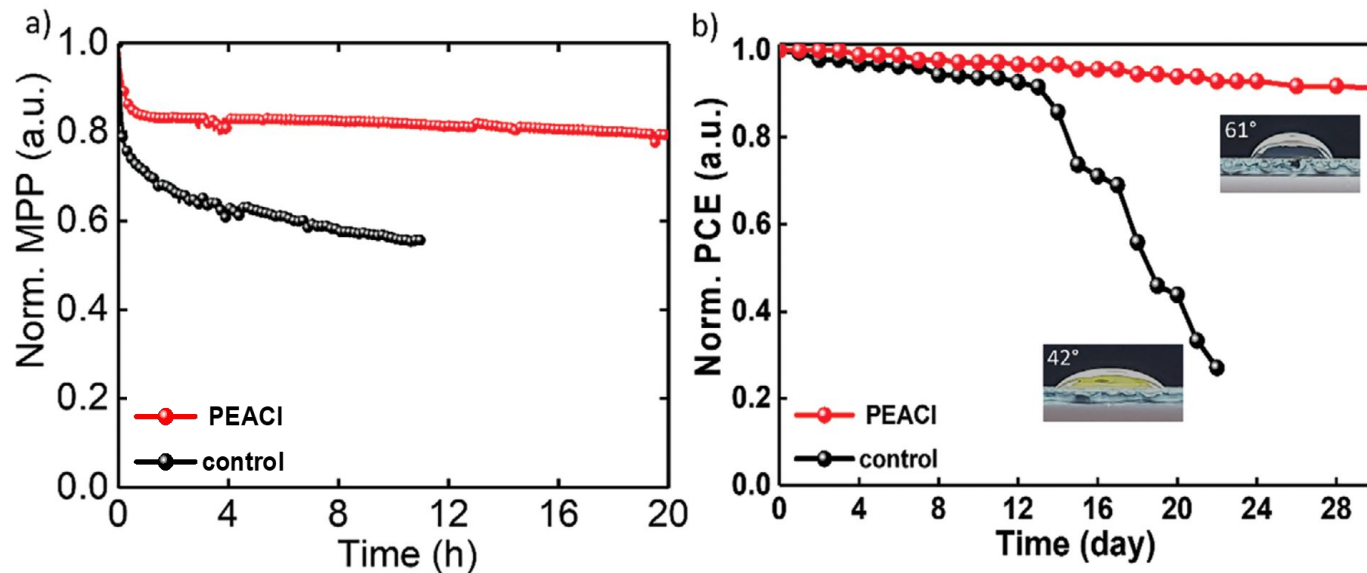
- PL & trPL: Lower density of grain boundaries lead to improved carrier lifetime, i.e. reduced non-radiative recombination rate



- jV : Reduced non-radiative recombination improves V_{oc} & FF

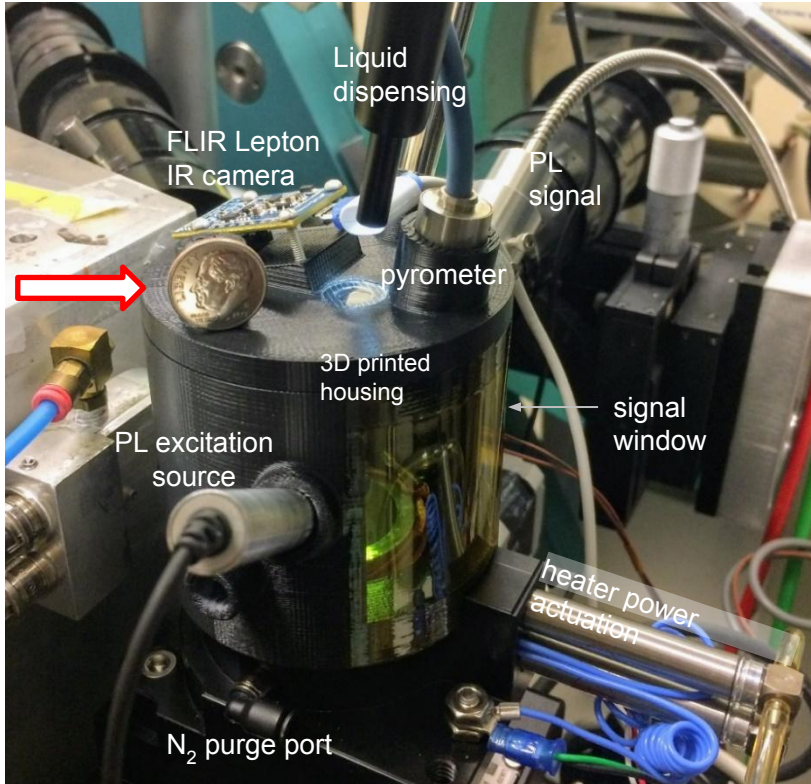


How does the integrated procedure compare to the 2-step deposition?



- Simplified, integrated one-step growth/passivation still stabilizes the perovskite under both continuous operation conditions (left) and under humidity
 - Newly developed PEACI-Antisolvent-Treatment can improve efficiency & stability while reducing the deposition time & effort

User Program: The multimodal in situ spin-coater at BL12.3.2



- Automated spin-coating, heating, and liquid dispensing in variable atmosphere
- Multimodal in situ photoluminescence and X-ray diffraction measurements
- Real time data acquisition (< 1s time resolution)
- Easy user operation (4 hours training)
- Fairly high throughput (~10 runs/shift)
- Compact and modular design
- Available to users since 2023

Successful User Program

Collaborations since 2023:

- [1] T. Kodalle, et al. **Adv. Ener. Mater.** vol 13, no. 33, p. 2201490, 2023.
- [2] M. Ralaiarisoa, et al. **Small Methods**, vol. 7, no. 11, p. 2300458, 2023.
- [3] P. Shi et al., **Nature**, vol. 620, pp. 323-327, 2023.
- [4] M. Singh, et al., **ACS Chem. Mater.**, vol. 35, no. 18, pp. 7450-7459, 2023.
- [5] W. Zuo, et al., **Adv. Mater.**, vol. 35, no. 39, p. 2302889, 2023.
- [6] M. G. D. Guita, et al., **Adv. Funct. Mater.**, Early View, p. 2307104, 2023.
- [7] K. Park, et al. **Adv. Mater.** vol. 36, no. 14, p. 2307265, 2024.
- [8] L. Scalon, et al., **Adv. Optical Mater.**, vol. 12, no. 2, p. 2300776, 2024.
- [9] T. Kodalle et al., **Adv. Mater.** vol. 36, no. 24, p. 2309154, 2024.
- [10] R. F. Moral, et al., **ACS Energ. Lett.**, vol. 9, no. 6, p. 2703-2716, 2024.
- [11] S. Sidhik, et al., **Science**, vol. 384, no. 6701, p. 1227-1235, 2024.
- [12] S. Wang, et al., **Small Science**, vol. 4, no. 12, p. 2400292, 2024.
- [13] L. Scalon, et al., **ACS Appl. Mat. & Interf.**, vol. 16, no. 38, p. 51727-51737, 2024.
- [14] M. G. D. Guita, et al., **Adv. Func. Mat.**, vol. 34, no. 50, p. 2307104, 2024.
- [15] P. E. Marchezi, et al., **J. Mat. Chem. A**, vol. 13, no. 22, p. 16671-16680, 2025.
- [16] M. G. D. Guita, et al., **Solar RRL**, p. 202500404, 2025.
- [17] Y. Zhang, et al., **Science**, vol. 387, no. 6731, p. 284-290, 2025.
- [18] K. Datta, et al., **Nature Comm.**, vol. 16, no. 1, p. 1967, 2025.
- [19] M.-C. Shih, et al., **Adv. Mat.**, vol. 37, no. 17, p. 2416672, 2025.
- [20] S. Liu, et al., **J. Amer. Chem. Society**, vol. 147, no. 19, p. 16681-16693, 2025.
- [21] S. Tan, et al., **Science**, vol. 388, no 6747, p. 639-645, 2025



University of Stuttgart
Germany



Thank you for your attention!

Funding Acknowledgement

The logo for the Deutsche Forschungsgemeinschaft (DFG), consisting of the letters 'DFG' in a bold, blue, sans-serif font.

Deutsche
Forschungsgemeinschaft



U.S. DEPARTMENT OF
ENERGY

Office of Science

PIs and Main Collaborators



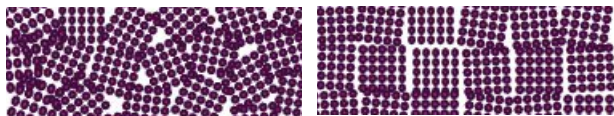
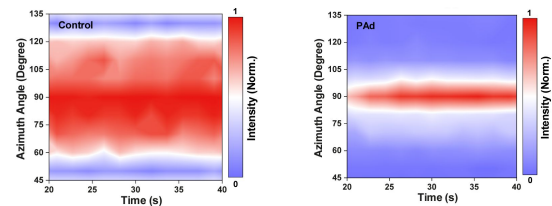
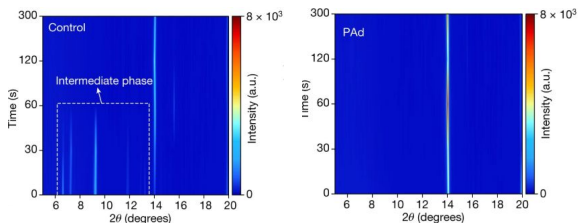
Universität
Stuttgart



Some Perovskite Highlights

Compositional engineering of film adhesion and roughness

Correlation of intermediate phase formation and crystal orientation

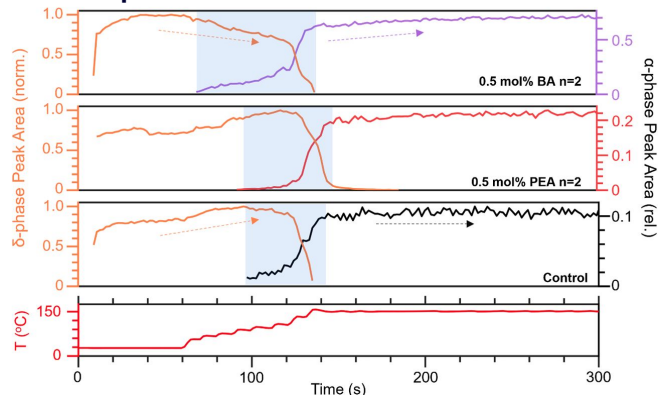


Random Orientation

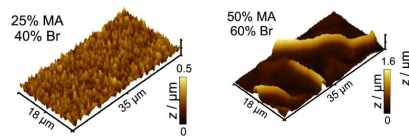
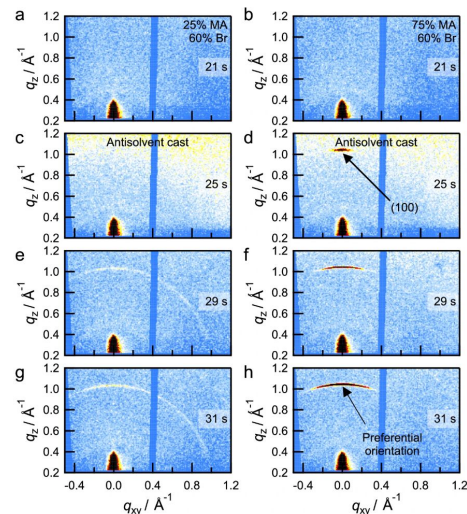
Preferential Orientation

P. Shi, T. Kodalle, et al., Nature 620 (7973), 323-327, 2023.

Controlling phase transitions via precursor additives



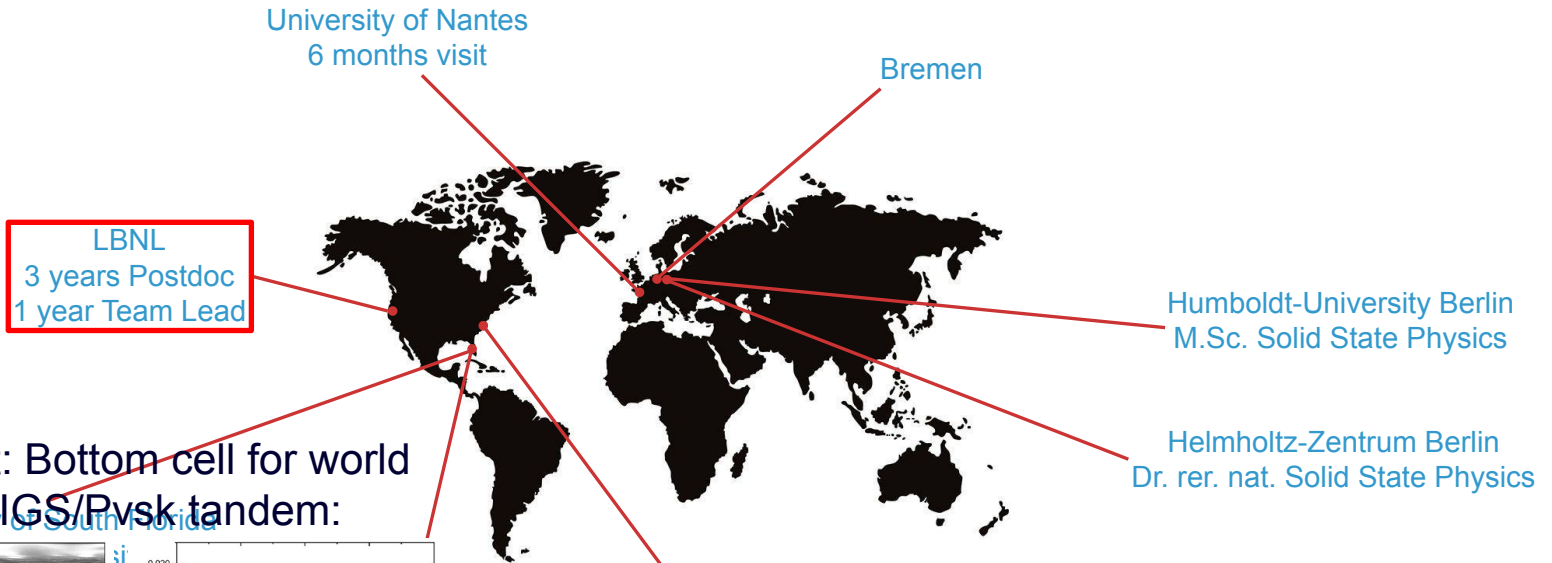
S. Sidhik, I. Metcalf, T. Kodalle, et al., Science 384 (6701), 1227-1235, 2024.



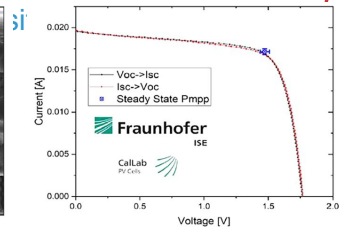
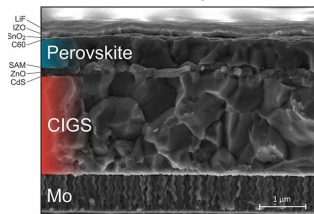
K. Datta, T. Kodalle, et al., Nature Comm. 16 (1967), 2025.



Things I've done in the (academic) world



Highlight: Bottom cell for world record CIGS/Perovskite tandem:



M. Jost, T. Kodalle, et al., ACS Energy Letters 7(4), 2022.